Document Number**:** H2020-EUK-815323/5G-ALLSTAR/D3.3

Project Name:
5G AgiLe and fLexible integration of SaTellite And cellulaR (5G-ALLSTAR)

Deliverable D3.3

Interference mitigation techniques

Date of delivery:	09/10/2020	Version:	1.0
Start date of Project:	01/07/2018	Duration:	36 months

Deliverable D3.3
Interference mitigation techniques

Project Number:	H2020-EUK-815323
Project Name:	5G AgiLe and fLexible integration of SaTellite And cellu-laR

Document Number:	H2020-EUK-815323/5G-ALLSTAR/D3.3
Document Title:	Interference mitigation techniques
Editor(s):	Jean-Michel Houssin (TAS)
Authors:	Nicolas Cassiau (CEA), Jean-Michel Houssin (TAS), Gosan Noh (ETRI) Additional authors from Chungnam National University under subcontract agreement with ETRI: Bang Chul Jung, Jeong Seon Yeom
Dissemination Level:	PU
Contractual Date of Delivery:	09/10/2020
Security:	Public
Status:	Final
Version:	1.0
File Name:	5G-ALLSTAR_D3.3.docx

Abstract

This deliverable has been created as part of the work in the project 5G-ALLSTAR Work Package 3 on Spectrum Sharing. It reports proposed beamforming and signal processing techniques as well as radio resource management schemes, and the study of their performance for mitigation of interferences caused by multiple radio (including satellite) access technologies sharing the same spectrum.

Keywords

Interference mitigation, multi-RAT, Non terrestrial networks, physical layer, beamforming, radio resource management.

Acknowledgements

We would like to acknowledge the following people for the valuable reviews to the deliverable:

Leszek Raschkowski (Fraunhofer HHI).

Executive Summary

This deliverable presents beamforming and signal processing techniques as well as radio resource management schemes, and the study of their performance for mitigation of interferences caused by multiple radio (including satellite) access technologies sharing the same spectrum. Avenues explored include dual beamforming (combining Maximum Ratio Transmission and Zero Forcing beamforming), physical layer design (increasing out of band rejection), and Radio Resource Management techniques: (i) new design of an exclusion zone for the protection of the Earth station and (ii) Time, Frequency or Time*Frequency coordination schemes.

Contents

List of Figures

List of Tables

List of Abbreviations

2D	2 Dimensions / 2-Dimensional
3D	3 Dimensions / 3-Dimensional
3GPP	3rd Generation Partnership Project
ARQ	Automatic Repeat Request
AWGN	Additive White Gaussian Noise
CA	Carrier Aggregation
CC	Carrier Component
CDF	Cumulative Distribution Function
CIR	Carrier-to-Interference Ratio
CNIR	Carrier-to-Noise-and-Interference Ratio
CNR	Carrier-to-Noise Ratio
CP-OFDM	Cyclic-Prefix OFDM
DL	Downlink
eICIC	Enhanced ICIC. Based on Sub-frame scheduling coordination between base stations (eNB, gNB)
FDD	Frequency Division Duplexing
FRF	Fractional Re-use Frequency
FSS	Fixed Satellite Service
GEO	Geostationary Earth Orbit
GF	Geometry Factor
HARQ	Hybrid ARQ
ICI	Inter-Cell Interference
ICIC	Inter-Cell Interference Coordination. Based on PRB use coordination between base stations (eNB, gNB).
IoT	Internet of Things
ISD	Inter-site distance
KPI	Key Performance Indicator
LEO	Low Earth Orbit
LOS	Line-Of-Sight
MEO	Medium Earth Orbit
MRT	Maximum Ratio Transmission
MSS	Mobile Satellite Service
NA	Not Applicable
NLOS	Non-Line-Of-Sight
NTN	Non-Terrestrial Network. It covers Satellite systems and HAPS (High Altitude Platform Service) systems.
OFDM	Orthogonal Frequency Division Multiplexing
PCC	Primary Carrier Component
PDF	Probability Density Function
PFD	Power Flow Density.
PG	Path Gain
PRB	Physical Resource Block. Model shared by LTE-A (4G waveform) and NR (5G waveform).
QoS	Quality of Service
RBG	Radio Bearer Group. In RRM simulator, a DL RBG contains to 4 PRBs and an UL RBG contains 1 PRB.
RTT	Round Trip Time
Rx	Receiver / Reception
SCC	Secondary Carrier Component
SCS	Sub Carrier Spacing
SES	Satellite Earth Station
SINR	Signal-to-Interference-and-Noise Ratio
SIR	Signal-to-Interference Ratio
SNR	Signal-to-Noise Ratio
SRS	Sounding Reference Signal
SSA	Satellite Service Area. Equivalent to NTN cell.
TBD	To Be Decided
TDD	Time Division Duplexing
Tx	Transmitter / Transmission
UE	User Equipment
UL	Uplink
VSAT	Very Small Aperture Terminal
Wrt	With respect to
ZF	Zero Forcing

1 Introduction

In this document, 5G-ALLSTAR explores methods to decrease the interference inherent in multi-RAT systems, in particular in the mixed terrestrial/satellite systems of interest here.

Beamforming techniques, in section 2, can be helpful to mitigate interference between satellite and cellular networks. Considering a realistic coexistence scenario where the downlink resource of the satellite link is shared by the cellular network, a dual beamforming technique is proposed that can generate a transmit beamforming vector at the cellular base station so as to satisfy the allowable interference level at the satellite Earth station while improving the sum rate of the cellular network. In the dual beamforming scheme, maximum ratio transmission (MRT) and zero forcing (ZF) beamforming techniques are combined. Further enhancements can be achieved by adaptively allocating the allowable interference level to each base station.

As shown by simulation in deliverable D3.2 [14], the terrestrial signal is received at a much higher power level than the satellite signal. This can cause interference from the former to the latter, when the signals are adjacent in frequency. It is then necessary to introduce frequency guard bands between the two systems, causing a net loss of throughput. In section 3, we study the performance of filtered waveforms compatible with the 5G NR standard in order to reduce these guard bands.

An exclusion zone concept can be used as a means of interference limitation for the protection of the satellite Earth station in a satellite-cellular coexistence scenario, where resource allocation for the cellular base station can be done based on whether the base station is located within the exclusion zone radius or not. In order to improve the efficiency of the cellular network while sufficiently protecting the satellite Earth station, a non-circular-shaped exclusion region design scheme is proposed in section 4.1, which can adaptively allocate the exclusion zone radius based on the transmit and receive beam directions of the cellular base station and the satellite Earth station, respectively.

In section 4.2, an overview of mechanisms to mitigate interference between terrestrial RANs and NTN RAN, based on RRM coordination schemes is provided.

An RRM simulator has been developed for the assessment of one selected, implemented RRM scheme in section 4.3. The performance evaluation of this RRM scheme is discussed in 2.4 and 2.5. Recommendations towards the WP5 test bench are done in the RRM coordination schemes preliminary analysis.

2 Dual beamforming technique for interference mitigation

In this section, by employing dual beamforming at the cellular network, we introduce a way of enhancing the communication quality of the cellular network while limiting the aggregate interference from the cellular base stations to the satellite Earth station to a certain level.

2.1 Background

When a wireless device has multiple antennas, it can perform beamforming by exploiting the channel independence among the antennas. Thanks to this property, the channel gain for a specific channel can be reduced or amplified so as to eliminate the interference or maximize the signal strength, thereby boosting the overall cell capacity.

Using this property of the beamforming technique, several research attempts have been made to maximize the system performance while minimizing interference occurring when satellite and cellular systems share the same frequency band. A general framework for the satellite-cellular spectrum sharing system was provided in [1], which considered uplink/downlink transmission scenarios for the satellite and cellular systems, beamforming techniques at the cellular base station, and the coverage range between the cellular base station and the satellite Earth station. A study on the spectrum sharing between satellite and cellular systems were provided in [2], which revealed that the interference from the satellite Earth station to the cellular base station is more significant when the cellular network operates in the uplink. Beamforming and power control techniques for satisfying the interference condition at the satellite Earth station were proposed in [3]. Digital and analog beamforming techniques for limiting the interference to multiple satellite Earth stations to a certain level were investigated [4]. A beamforming technique for guaranteeing secrecy communication performance of the satellite and cellular links when an eavesdropper tries to eavesdrop the satellite signal [5]. In [6], a beamforming technique for maximizing the satellite link performance while minimizing the interference to the cellular UEs was provided.

In this section, considering a realistic satellite-cellular sharing scenario where both satellite and cellular links operate in the downlink, a beamforming vector design is provided for the cellular base station. The objective of the proposed beamforming technique is to maximize the communication performance while limiting the amount of maximum allowable interference at the satellite Earth station to a predefined level. More specifically, a combination of ZF beamforming using null space of the interference channel and MRT beamforming which can maximize the channel gain of the cellular link is provided.

2.2 System model

A spectrum sharing model of satellite and cellular networks is shown in Figure 2-1. A satellite Earth station receives a signal from a satellite using a directive antenna oriented towards the satellite. The elevation angle of the satellite is assumed to be 90°. The allowable interference level at the satellite Earth station is defined as Q.

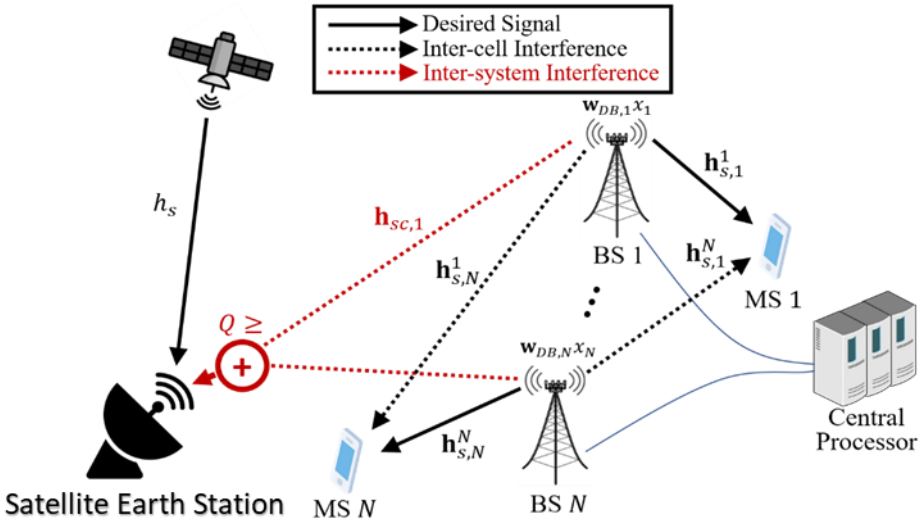

Figure 2-1: Spectrum sharing model of satellite and cellular networks

The antenna gain of the directive antenna is modeled according to the ITU-R S.465-5 recommendation [7], as follows:

$$G(\theta) = \begin{cases} 32 \text{ dBi} & |\theta| < 1° \\ 32 - 25\log\theta \text{ dBi} & 1° < |\theta| < 48° \\ -10 \text{ dBi} & 48° < |\theta| < 180° \end{cases}$$

A central processor within the cellular network, which is connected to all the base stations, is responsible for the allocation of the allowable interference level to the base stations. The number of base stations is N and each base station has K antennas. Each UE is assumed to have a single antenna. Each base station is required to be located farther than a preset distance of $D_{\min}$ from the satellite Earth station. The maximum distance between the satellite Earth station and the base stations is $D_{\max}$. The coverage radius of a cellular base station is assumed to be D_c. Each cellular base station is equipped with an array antenna so that it can perform beamforming.

The channel gain between the n-th base station and the m-th UE is denoted by $\mathbf{h}_{s,m}^n \in \mathbb{C}^{1\times K}$. The channel gain between the n-th base station and the satellite Earth station is denoted by $\mathbf{h}_{sc,n} \in \mathbb{C}^{1\times K}$. Assuming a mmWave frequency band, the above channel gains are given by

$$\mathbf{h}_{s,m}^n = \sqrt{\frac{K}{LP_{n,m}}} \sum_{l=1}^{L} \alpha_l^{[n,m]} \mathbf{a}\left(\theta_{T,l}^{[n,m]}\right)^H$$

$$\mathbf{h}_{sc,n} = \sqrt{\frac{K}{LP_n}} \sum_{l=1}^{L} G\left(\theta_{R,l}^{[n]}\right) \alpha_l^{[n]} \mathbf{a}\left(\theta_{T,l}^{[n]}\right)^H,$$

where L is the number of multipath components. $\alpha_l^{[n,m]}$ and $\alpha_l^{[n]}$ represent the refraction and reflection components and follow $CN(0,1)$ distribution. $\theta_{R,l}^{[n]}$ denotes the angle of arrival of the signal from the n-th base station propagated through the l-th path. $\theta_{T,l}^{[n,m]}$ and $\theta_{T,l}^{[n]}$ are the angles of departure of the signal transmitted from the n-th base station to the m-th UE and the satellite Earth station, respectively, propagated through the l-th path. $P_{n,m}$ and P_n are the path losses between the n-th base station and the m-th UE and between the n-th base station and the satellite Earth station, respectively:

$$P_{n,m} = d_{n,m}^{\beta}$$

$$P_n = d_n^{\beta}$$

where β is the path loss exponent. $d_{n,m}$ and d_n are the distances between the n-th base station and the m-th UE and between the n-th base station and the satellite Earth station, respectively. $\mathbf{a}(\theta)$ is the steering vector which can be written as

$$\mathbf{a}(\theta) = \left[1, e^{-j\pi\cos(\theta)}, \dots, e^{-j\pi(K-1)\cos(\theta)}\right]^T.$$

The interference from the cellular base stations to the cellular UE and satellite Earth station, respectively, can be expressed as

$$y_n = \mathbf{h}_{s,n}^n \mathbf{w}_n x_n + \sum_{m \neq n} \mathbf{h}_{s,n}^m \mathbf{w}_m x_m + z_n$$

$$y_{sc} = \sum_{n}^{N} \mathbf{h}_{sc,n} \mathbf{w}_n x_n + z_{sc}$$

where x_n is the transmitted signal from the n-th base station, and $\mathbf{w}_n$ is the transmit beamforming vector of the n-th base station. z_n and z_{sc} are the additive white Gaussian noise (AWGN) following $CN(0, \sigma_0^2)$.

The sum-rate of the cellular network is then defined as

$$R = \sum_{n=1}^{N} \log_2\left(1 + \frac{\left|\mathbf{h}_{s,n}^n \mathbf{w}_n\right|^2}{\sigma_0^2 + \sum_{m \neq n}\left|\mathbf{h}_{s,n}^m \mathbf{w}_m\right|^2}\right).$$

The interference limit condition is given by

$$\sum_{n=1}^{N}\left|\mathbf{h}_{sc,n}\mathbf{w}_n\right|^2 P_T \leq Q.$$

where P_T denotes the transmit power of the base station.

2.3 Dual beamforming technique based on interference threshold

The proposed dual beamforming technique consists of three steps: 1) interference threshold-based base station ON/OFF control, 2) allocation of allowable interference level, and 3) generation of combined transmit beamforming vectors.

2.3.1 Interference threshold-based base station ON/OFF control

Although the interference can be suppressed to a certain extent by employing both the MRT and ZF beamforming, the overall efficiency can be degraded when the amount of interference from the cellular base station to the satellite Earth station is significantly high. This is because, in this case, the base station has to only rely on the ZF beamforming which enables interference-free transmission to the satellite Earth station, while not taking advantage of utilizing MRT beamforming to improve its own signal quality.

Hence, in the first step of the proposed dual beamforming scheme, for each base station, the portion of the beamforming vector which can be used for the MRT beamforming is calculated. Then, if this calculated value is less than a preset amount, the base station is turned off so as to avoid interference and reduce power consumption.

The detailed algorithm for the interference threshold-based base station ON/OFF control is summarized in Table 2-1. Here, Q_n' means the temporarily allocated allowable interference level in order to decide whether to turn the base station on or off. ϵ_{th} is the MRT beamforming ratio condition and is determined based on the sum rate of the base station and the interference level to the satellite Earth station. ϵ_n is the MRT beamforming ratio condition for the temporarily allocated n-th base station, which is inversely proportional to the transmit power.

Table 2-1: Description of Algorithm 1

Algorithm 1: Interference threshold-based base station ON/OFF control
1: Initialize: $Q'_n = Q/N$, $\mathbf{w}_{\mathrm{MRT},n} = \left(\mathbf{h}_{s,n}^n\right)^H / \left\|\mathbf{h}_{s,n}^n\right\|$ $(n \in \{1, \dots N\})$, $\epsilon_{th} = 1/(1+P_T)$
2: Calculate beamforming ratio: $\epsilon_n = \min\left(1, Q'_n / \left(P_T \left|\mathbf{h}_{cs,n}\mathbf{w}_{\mathrm{MRT},n}\right|^2\right)\right)$
3: Turned base station ON/OFF according to $O = \{n \mid \epsilon_{th} < \epsilon_n\}$

Figure 2-2 depicts an example of base station ON/OFF control procedure. If the amount of interference from a specific base station (e.g., BS 1 or BS N) is too large, the base station is turned off since it cannot obtain a favorable MRT beamforming vector.

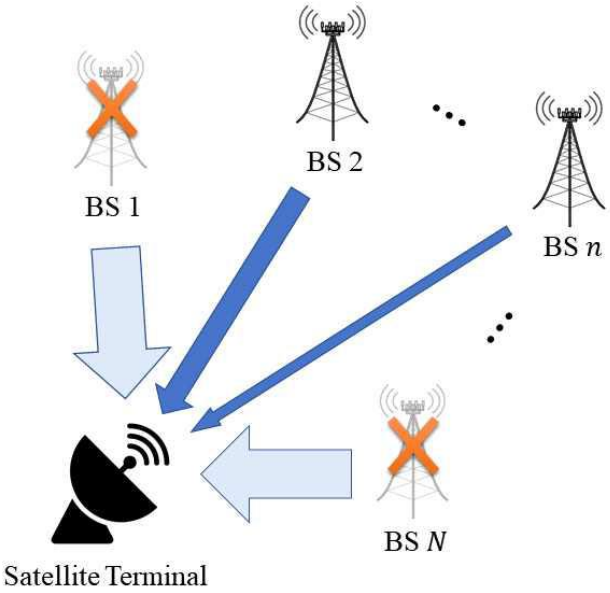

Figure 2-2: Example of base station ON/OFF control

2.3.2 Allocation of allowable interference level

The total allowable interference level at the satellite Earth station can be satisfied by properly allocating the part of the total allowable interference level to each base station and then by locally satisfying the allocated allowable interference level. As discussed above, some base stations can be turned off when they induce excessive interference to the satellite Earth station. In contrary, a base station may cause low interference to the satellite Earth station, thereby leaving a large portion of the allocated allowable interference level unused. If the unused portion of the allowable interference level can be reallocated to other base stations, the sum rate of the cellular network can be improved while still sufficiently protecting the satellite Earth station.

The proposed algorithm for the allocation of the allowable interference level is described in Table 2-2. The algorithm is performed at the central processor after collecting required information such as channel state information and the overall allowable interference level. After the execution of the algorithm, the allowable interference level is distributed to each base station.

Table 2-2: Description of Algorithm 2

Algorithm 2: Allocation of allowable interference level

1: Initialize: $Q_n = Q/N$, $\mathbf{w}_{\mathrm{MRT},n} = \left(\mathbf{h}_{s,n}^n\right)^H / \left\|\mathbf{h}_{s,n}^n\right\|$ $(n \in \{1, \dots N\})$

2: **do**

3: Obtain sets: $R = \left\{n | P_T \left|\mathbf{h}_{cs,n}\mathbf{w}_{\mathrm{MRT},n}\right|^2 \le Q_n\right\}$, $E = \left\{n | P_T \left|\mathbf{h}_{cs,n}\mathbf{w}_{\mathrm{MRT},n}\right|^2 > Q_n\right\}$

4: Calculate: $Q_{res} = \sum_{n \in R} Q_n - P_T \left|\mathbf{h}_{cs,n}\mathbf{w}_{\mathrm{MRT},n}\right|^2$

5: Calculate: $Q_n = Q_n + Q_{res}/|E|$, $(n \in E)$

6: **while** $|R| > 0$ **end**

Figure 2-3 shows an example of the algorithm operation. The procedure of distributing allowable interference among the base stations is repeated until every base station satisfies its allowable interference level.

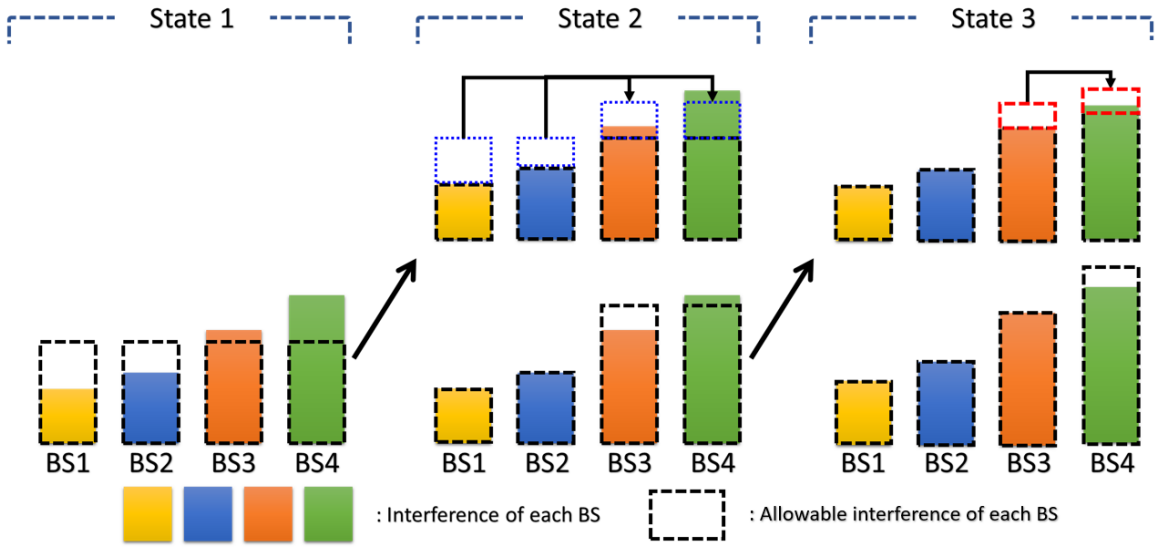

Figure 2-3: Example of allocation of allowable interference level

2.3.3 Generation of transmit dual beamforming vectors

In the considered system, MRT beamforming is used to maximize the throughput between the cellular base station and UE. However, employing only MRT beamforming without considering interference mitigation may incur significant interference to the satellite Earth station. When the transmitter has more antenna than the receiver, a null space of size equal to the difference of the number of antennas between the transmitter and receiver can be constructed. Using this null space, ZF beamforming can be additionally employed to nullify the interference to the satellite Earth station.

In the proposed dual beamforming technique, a combined beamforming vector is generated by adding the MRT beamforming vector with reduced magnitude and the ZF beamforming vector such that the overall beamforming vector has a unit magnitude. The proposed dual beamforming algorithm is summarized in Table 2-3.

Table 2-3: Description of Algorithm 3

Algorithm 2: Generation of transmit dual beamforming vectors

1: Obtain: $\mathbf{w}_{\mathrm{MRT},n} = \left(\mathbf{h}_{s,n}^{n}\right)^{H} / \left\|\mathbf{h}_{s,n}^{n}\right\|, \rho_{\mathrm{MRT},n} = \min\left(1, \frac{Q}{P_T \left|\mathbf{h}_{cs,n}\mathbf{w}_{\mathrm{MRT},n}\right|^2}\right), \ (n \in \{1, \dots N\})$

2: Obtain: $\mathbf{W}_{\mathrm{ZF},n} = \mathrm{null}\left(\mathbf{h}_{cs,n}\right) = \left[\mathbf{w}_{\mathrm{ZF},n}^{(1)}, \dots, \mathbf{w}_{\mathrm{ZF},n}^{(K-1)}\right] \in \mathbb{C}^{K\times(K-1)}$

3: Calculate BF vector portion: $\rho_{\mathrm{ZF},n}^{(k)} = \left(-b_n^{(k)} + \sqrt{b_n^{(k)2} - a_n^{(k)} c_n^{(k)}}\right)^2 \Big/ a_n^{(k)2}$

where $a_n^{(k)} = \left\|\mathbf{w}_{\mathrm{MRT},n}\right\|^2$,

$b_n^{(k)} = \sqrt{\rho_{\mathrm{MRT},n}}\left(\mathrm{Re}\left(\mathbf{w}_{\mathrm{MRT},n}^{T}\right)\mathrm{Re}\left(\mathbf{w}_{\mathrm{ZF},n}^{(k)}\right) + \mathrm{Im}\left(\mathbf{w}_{\mathrm{MRT},n}^{T}\right)\mathrm{Im}\left(\mathbf{w}_{\mathrm{ZF},n}^{(k)}\right)\right)$,

$c_n^{(k)} = \rho_{\mathrm{MRT},n}\left\|\mathbf{w}_{\mathrm{MRT},n}\right\|^2 - 1$

4: Select: $k^* = \arg\max_k \left\|\mathbf{h}_{s,n}^{n}\left(\mathbf{w}_{\mathrm{MRT},n}\sqrt{\rho_{\mathrm{MRT},n}} + \mathbf{w}_{\mathrm{ZF},n}^{(k)}\sqrt{\rho_{\mathrm{ZF},n}^{(k)}}\right)\right\|^2$

5: Calculate: $\mathbf{w}_{n,t} = \mathbf{w}_{\mathrm{MRT},n}\sqrt{\rho_{\mathrm{MRT},n}} + \mathbf{w}_{\mathrm{ZF},n}^{(k^*)}\sqrt{\rho_{\mathrm{ZF},n}^{(k^*)}}$

6. Decide: $\mathbf{w}_n = \begin{cases} \mathbf{w}_{\mathrm{MRT},n}\sqrt{\rho_{\mathrm{MRT},n}} & \left\|\mathbf{h}_{s,n}^{n}\mathbf{w}_{n,t}\right\|^2 < \left\|\mathbf{h}_{s,n}^{n}\mathbf{w}_{\mathrm{MRT},n}\sqrt{\rho_{\mathrm{MRT},n}}\right\|^2 \\ \mathbf{w}_{n,t} & \left\|\mathbf{h}_{s,n}^{n}\mathbf{w}_{n,t}\right\|^2 > \left\|\mathbf{h}_{s,n}^{n}\mathbf{w}_{\mathrm{MRT},n}\sqrt{\rho_{\mathrm{MRT},n}}\right\|^2 \end{cases}$

In the above proposed algorithm, $\rho_{\mathrm{MRT},n}$ is the portion of the MRT beamforming vector employed by the n-th base station, which is dependent on the allowable interference level allocated to that base station. In order to achieve higher gain by the dual beamforming compared to that by the MRT beamforming, a suitable portion between the MRT and ZF beamforming need to be calculated. In the algorithm, procedure 6 enables to decide whether to employ the ZF beamforming in addition to the MRT beamforming.

2.4 Simulation results

The proposed dual beamforming scheme is verified via computer simulation. The performance of the proposed dual beamforming is compared with the beamforming schemes based only on either MRT beamforming or ZF beamforming.

Figure 2-4 and Figure 2-5 show the sum rate of the cellular network as a function of the number of base station antennas for $N = 10$ and $N = 20$, respectively. It is seen that the proposed dual beamforming technique outperforms both MRT and ZF beamforming schemes. In addition, the sum rate increases as the number of base stations increases.

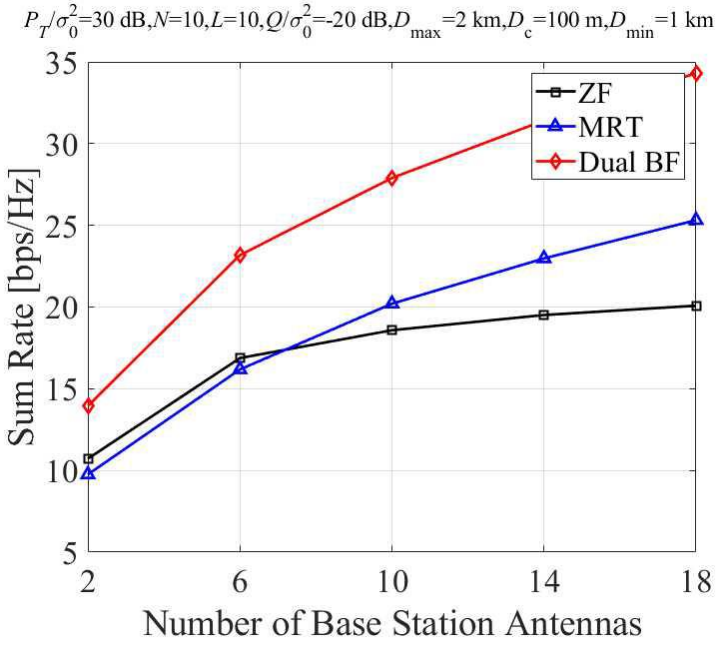

Figure 2-4: Sum rate vs. Number of base station antennas ($N = 10$)

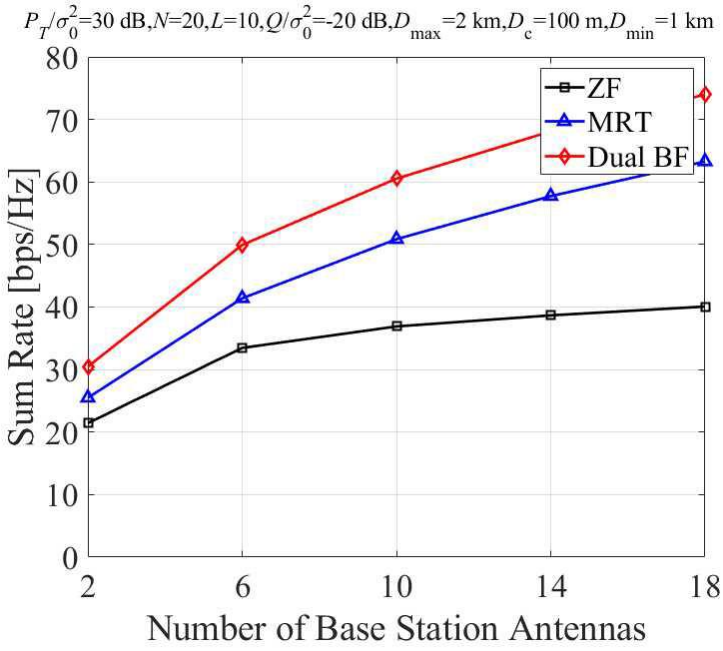

Figure 2-5: Sum rate vs. Number of base station antennas ($N = 20$)

Figure 2-6 and Figure 2-7 show the sum rate of the cellular network as a function of the interference constraint for different transmit powers of $P_T/\sigma_0^2 = 20$ dB and $P_T/\sigma_0^2 = 30$ dB, respectively. It is seen that the sum rates of the dual beamforming and MRT beamforming converge as the interference constraint increases. In contrast, for low interference constraint values, the sum rate of the dual beamforming converges to that of the ZF beamforming. With large P_T/σ_0^2 value, the sum rate of the ZF beamforming is significantly increased.

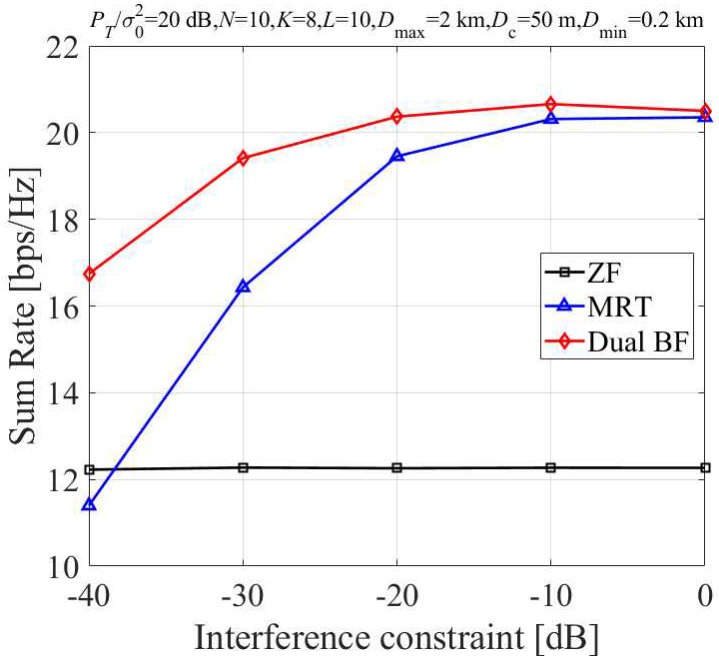

Figure 2-6: Sum rate vs. Interference constraint ($P_T/\sigma_0^2 = 20$ dB)

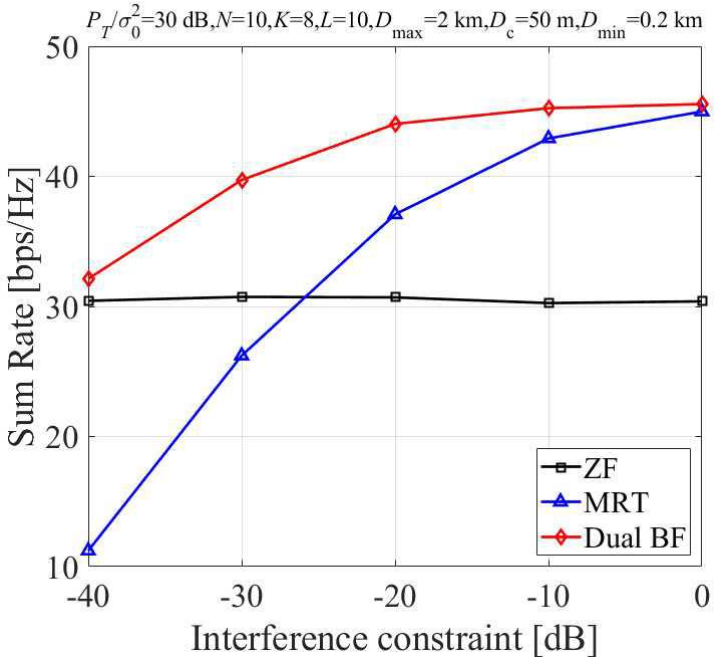

Figure 2-7: Sum rate vs. Interference constraint ($P_T/\sigma_0^2 = 30$ dB)

2.5 Conclusion

This section proposed a dual beamforming technique to mitigate interference for the coexistence of the satellite and cellular networks. Each base station employs MRT beamforming which can incur interference levels lower than the allowable level, and also employs ZF beamforming for the further sum rate improvement as well as the interference mitigation. Since the expected interference level from each base station is different, adaptive allocation of the allowable interference level can further improve the sum rate of the cellular network. The performance enhancement by the dual beamforming is verified by the computer simulation, by comparing with the MRT and ZF-only beamforming schemes.

3 Signal processing techniques for active interference mitigation

In D3.2 [14], we have shown that the use of non-filtered CP-OFDM waveform for a terrestrial system adjacent in frequency to a satellite system implies using huge guard-bands between both bands to prevent interference from the terrestrial system on the satellite system. We therefore investigate in this section the use of filtered waveforms for mitigating this interference. It is important to note that contrary to LTE, 5G NR does not preclude the use of filtering techniques at the transmitter side, as long as it is transparent to the receiver and as the waveform is OFDM-based [16].

3.1 Description of waveforms

3.1.1 Filtered-OFDM

Filtered-OFDM (F-OFDM) consists in digitally filtering the signal at the output of the baseband transmitter. By doing so, the out-of-band (OoB) rejections of the waveform can be controlled and increased to the desired level, provided the adequate filter is used. The counterpart of this method is the space occupied by the filter in the hardware implementation, space which is all the more important as the order of the filter is high.

In this study we have used a 512-order truncated sinus cardinal filter, which magnitude response is show on Figure 3-1. Figure 3-3 plots the spectrum of F-OFDM, compared to the other studied waveforms.

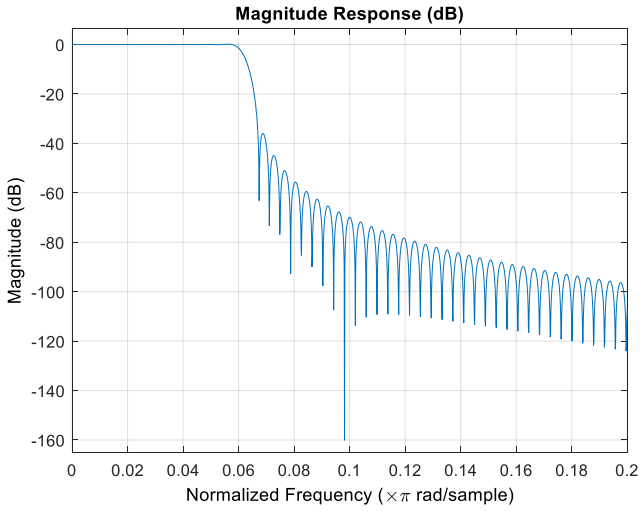

Figure 3-1: Magnitude response of the Filtered-OFDM digital filter.

3.1.2 Block Filtered-OFDM

Block Filtered-OFDM (BF-OFDM) was first introduced in 2017 in [17]. It is an improved version of FFT-FBMC [18] in the sense that the receiver can be reduced to a simple FFT and is therefore specification transparent. The proposed waveform provides a good spectral localization with enhanced side lobes rejection while providing equivalent performance against frequency selective channels compared to CP-OFDM and satisfies the complex quasi-orthogonality (very low level of intrinsic interference). Moreover, it excels in multi-user scenarios [19] and is fully flexible.

Figure 3-2 shows the BF-OFDM transmitter. The receiver, not shown, actually corresponds to a CP-OFDM receiver. The transmitter is composed of a filter bank fed by M CP-OFDM modulators operating in parallel. A framing stage maps $N/2$ OFDM sub-carriers in order to respect an intra-carrier orthogonality condition. An additional pre-distortion stage compensates the distortion introduced by the filter at the transmitter side.

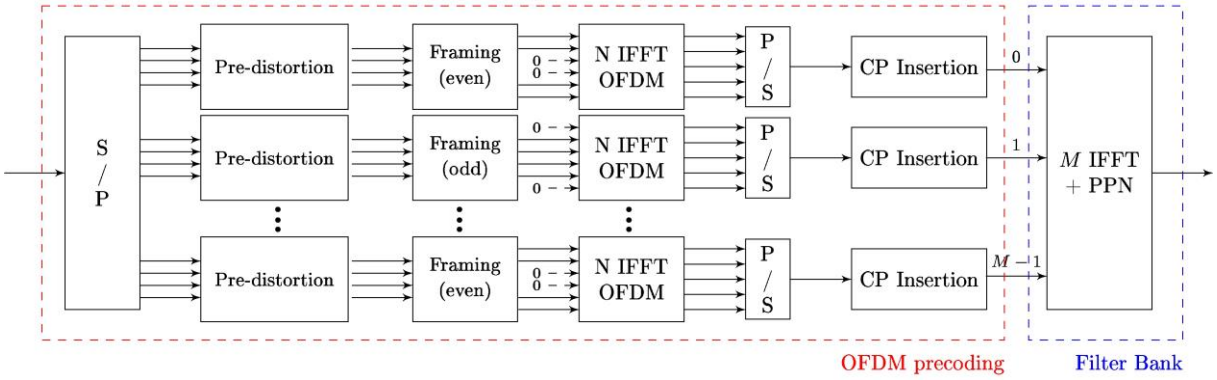

Figure 3-2: Block-Filtered-OFDM transmitter.

In [17], the following performance indicators of BF-OFDM are analyzed, results are summarized below:

- Spectral efficiency (SE). The proposed scheme achieves a SE very similar to the legacy CP-OFDM. In both cases, there is a spectral loss induced by the insertion of a Cyclic-Prefix (CP). Considering lower overlapping factor K of the filter bank (which relaxes the circularity condition and minimal CP size), is an efficient way to enhance the SE. In that case the level of interferences needs to be managed (see below *Signal to Interference Ratio*).
- Signal to Interference Ratio (SIR). The SIR is a key indicator as it is directly related to the quasi-orthogonality condition of the waveform, hence to the frequency response of the filter. BF-OFDM provides SIR in the order of 60 dB when combined with PHYDIAS filter shape, and even more, around 85 dB, if considering Gaussian filter for example.
- Complexity. Rather than counting the complex multiply necessary to perform the transmitter, we aim at proving that BF-OFDM can be implemented in hardware: in Work Package 5, we are therefore designing the transmitter in Hardware Description Language (HDL) and implementing the design in a Field Programmable Gate Array (FPGA). At the time this deliverable is published, we are confident that the whole transmitter (except Forward Error Coding) can be integrated in the FPGA of a Xilinx ZCU111 board.
- Power spectral density (PSD). PSD is the main indicator for the present study, as it indicates how efficiently the waveform can use the spectrum bandwidth without interfering with systems using adjacent bands. The filtering stage of BF-OFDM allows a very good frequency localization of each of the M OFDM modulated lines (see Figure 3-2), as shown on Figure 3-3. It is to be noted that this filtering is much less complex than the filtering stage of F-OFDM.

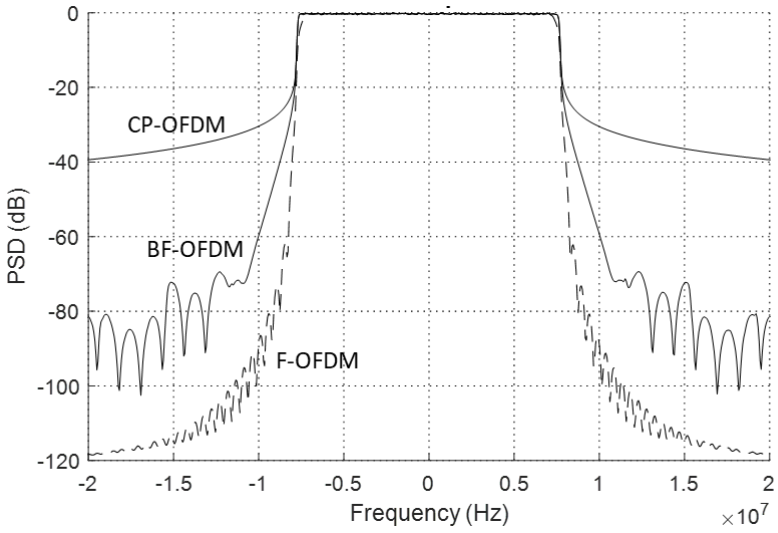

Figure 3-3: Out-of-band rejections of CP-OFDM, BF-OFDM and Filtered-OFDM.

3.2 Scenario and parameters

The scenario is the same than in D3.2 [14], except that here, performance of F-OFDM and BF-OFDM are also assessed. It is recalled on Figure 3-4: the impact of guard bands and relative cellular received power (ΔP) on the error rate of the satellite system are measured.

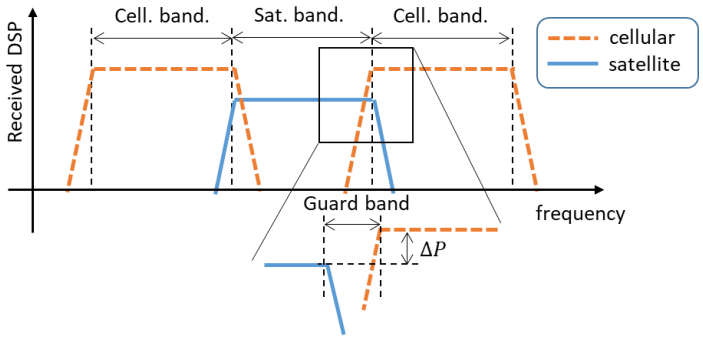

Figure 3-4: Simulated scenario and parameters.

Other parameters are:

- The channel models reflect the simulated environment, i.e. highway: the terrestrial channel model is TDL-D 100 as defined in [8], and the satellite channel model is Vehicular Open Rural with a K-Factor of 20 dB. The receiver speed is 110 km/h, the Doppler is simulated based on the sum of sinusoids method.
- The carrier frequency, 22.5 GHz, is consistent with the simulations from D3.1 [13].
- The terrestrial system uses numerology 2; for the satellite system numerologies 2 and 3 are assessed. For each 5G NR numerology, the inter-carrier spacing Δ_f, the OFDM symbol duration T_u^{μ}, the cyclic prefix duration T_{CP}^{μ} and the number of slots per frame $N_{slot}^{frame,\mu}$ are recalled in Table 3-1.

Table 3-1: 5G NR numerologies

μ	Δ_f $[kHz]$	T_u^{μ} $[\mu s]$	T_{CP}^{μ} $normal$ $[\mu s]$		
			$l = \{0, 7 \cdot 2^{\mu}\}$*	$l \neq \{0, 7 \cdot 2^{\mu}\}$*	$N_{slot}^{frame,\mu}$
0	15	66.66	5.21	4.69	10
1	30	33.33	2.86	2.34	20
2	60	16.66	1.69	1.17	40
3	120	8.33	1.11	0.59	80
4	240	4.16	0.81	0.29	160

* l is the OFDM symbol number in a subframe (1 ms).

- In adjacent channel systems, the interference is maximal on the spectrum edges; we can therefore expect the performance to vary with the width of the bandwidth. The performance is then evaluated with two bandwidths: 15.36 MHz and 30.72 MHz.
- The terrestrial Modulation and Coding Scheme (MCS) is #22 (64-QAM rate 666/1024). A range of MCS are assessed for the satellite system: #5 (QPSK 379/1024), #10 (16-QAM 340/1024) and #15 (16-QAM 616/1024).
- The guard band ranges from 0 kHz to 960 kHz.
- In order to reflect the differences between the terrestrial and the satellite received powers, the parameter ΔP is set to {15, 10, 5, 0} dB.

These parameters are summarized in Table 3-2.

Table 3-2: Adjacent channel interference parameters

Waveform	**CP-OFDM**	**F-OFDM**	**BF-OFDM**
Scenario	Highway		
Fc	22.5 GHz		
μ satellite	{2,3}		
μ cellular	2		
Satellite bandwidth	{15.36, 30.72} MHz		
Cellular bandwidth	{15.36, 30.72} MHz		
MCS satellite	{15, 10, 5}*		
MCS cellular	22*		
Guard band	{0,60,120,240,480,960} kHz		
Cellular on Satellite received power ΔP	{15,10,5,0} dB		
Channel satellite	Veh. open rural, K=20 dB		
Channel cellular	TDL-D 100**		
Speed	110 km/h		
Filter	N/A	Truncated sinc, order 512	PHYDIAS, overlapping factor 3

* **MCS 5**: QPSK 379/1024; **MCS 10**: 16-QAM 340/1024; **MCS 15**: 16-QAM 616/1024; **MCS 22**: 64-QAM 666/1024
** 3GPP TR 38.901 V14.2.0 (2017-09), [8]

Two metrics are used for performance assessment: The Packet Error Rate (PER) at the satellite receiver and the throughput loss due to guard bands. The PER is defined as the ratio between the number of correctly decoded slots on the total number of transmitted slots. The numbers of slots per frame are recalled in Table 3-1. Due to the long Round Trip Time (RTT) in satellite systems, the retransmission of badly decoded packets using Automatic Repeat Request (ARQ) may be not always possible. The PER at the first (and unique) transmission must therefore be very low. In this study we set the target PER to 10^{-3}.

3.3 Simulation results

Figure 3-6 to Figure 3-17 present the PER reached by the satellite receiver, depending on the relative interferer power (x-axis) and on the guard bands between the satellite and the cellular systems (y-axis). The value of the PER is given by the colour of the surface, as specified by Figure 3-5. PER=10^{-3} is the PER reached by the cellular receiver without interference.

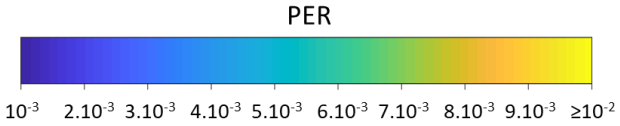

Figure 3-5: scale of Figure 3-6 to Figure 3-17.

3.3.1 15.36 MHz bandwidth

Figure 3-6 to Figure 3-11 are for a satellite bandwidth of 15.36 MHz. In this scenario, the throughput loss caused by possible guard bands is given in Table 3-3.

Table 3-3: Throughput loss due to guard bands for the 15.36 MHz bandwidth scenario

Guard band (each side), kHz	Throughput loss, %
0	0.00
60	0.78
120	1.56
240	3.12
480	6.25
960	12.50

For satellite MCS 15, F-OFDM and BF-OFDM perform nearly the same, and improve the performance compared to CP-OFDM. With this latter waveform, a correct PER can be reached only for a very low interferer power (0 dB) and with high guard bands (960 kHz). By using filtered waveforms, guard bands are no longer necessary, but the interferer power must still be limited. In all the cases, performance are better with numerology 2 than with numerology 3: with the former numerology, the proportion of carriers impacted is lower than with the latter.

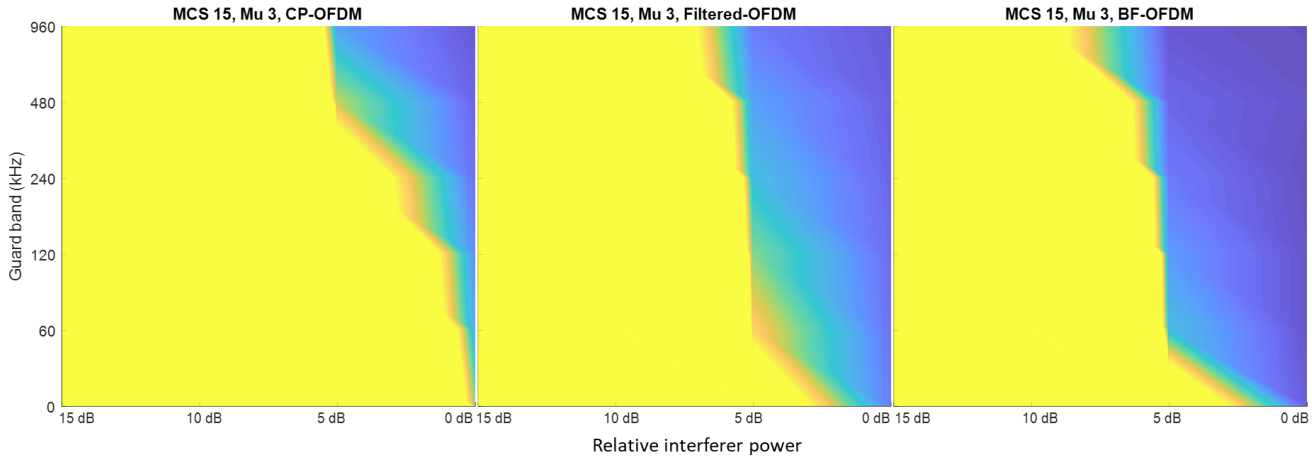

Figure 3-6: PER for MCS 15, μ=3, 15.36 MHz bandwidth. See scale on Figure 3-5.

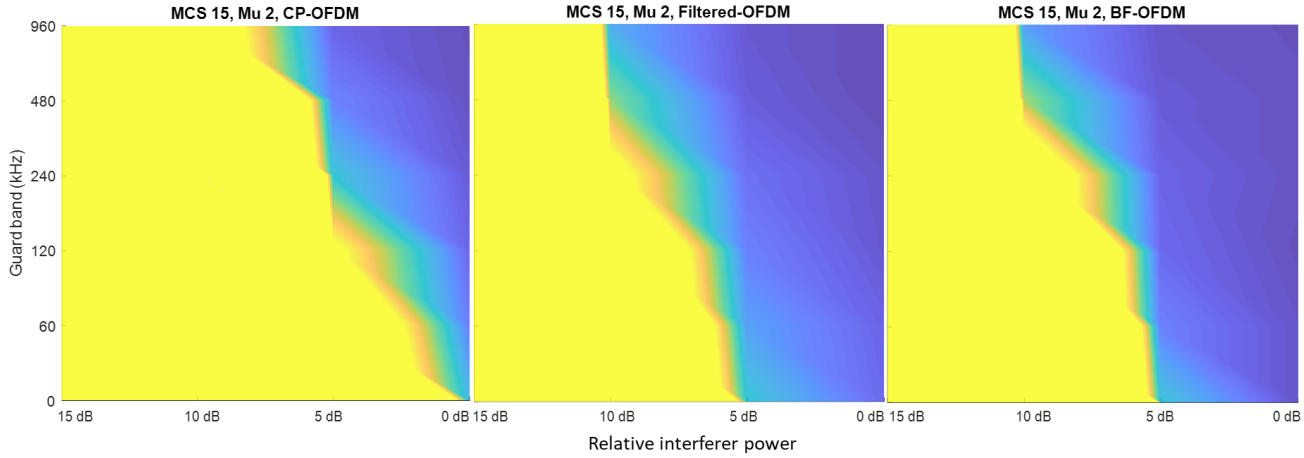

Figure 3-7: PER for MCS 15, μ=2, 15.36 MHz bandwidth. See scale on Figure 3-5.

For satellite MCS 10, BF-OFDM performs better than F-OFDM (specially for numerology 2), and both are more efficient than CP-OFDM. With CP-OFDM, small guard bands are possible only for a very low power interferer (<5 dB). By using BF-OFDM, limited guard bands (120 kHz) can be used even for a high power interferer (around 10 dB). Once again, in all the cases, performance is better with numerology 2 than with numerology 3. With numerology 2, very high power interferer (15 dB) can be managed by BF-OFDM, but at the cost of high guard bands (240 kHz).

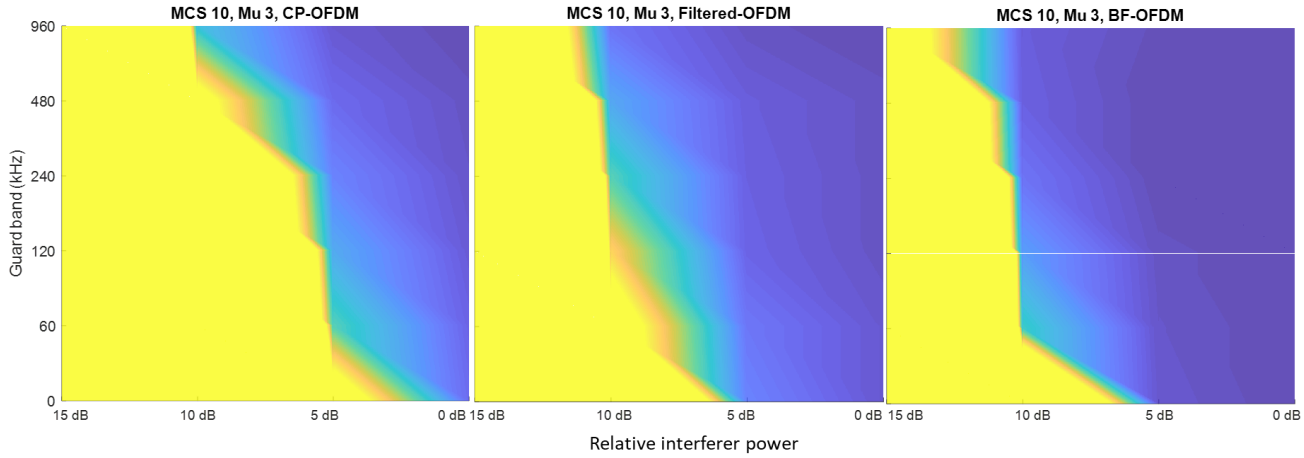

Figure 3-8: PER for MCS 10, μ=3, 15.36 MHz bandwidth. See scale on Figure 3-5.

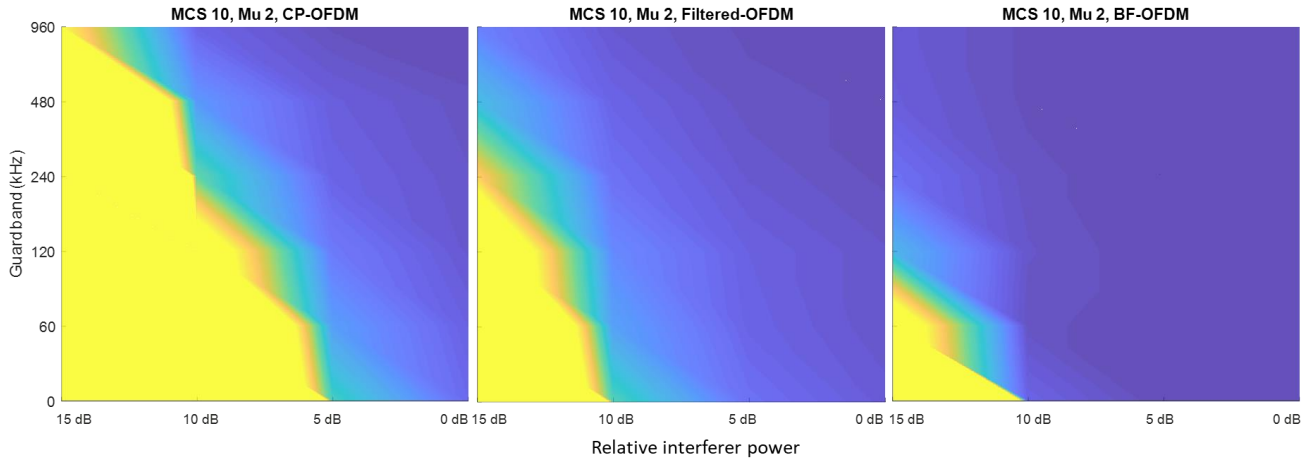

Figure 3-9: PER for MCS 10, μ=2, 15.36 MHz bandwidth. See scale on Figure 3-5.

For satellite MCS 5, the most robust, BF-OFDM performs a bit better than F-OFDM, and both are more efficient than CP-OFDM. With CP-OFDM, small guard bands are possible only for a very low power interferer (<5 dB). By using BF-OFDM, limited guard bands (120 kHz) can be used even for a high power interferer (around 10 dB). Once again, in all the cases, performance is better with numerology 2 than with numerology 3.

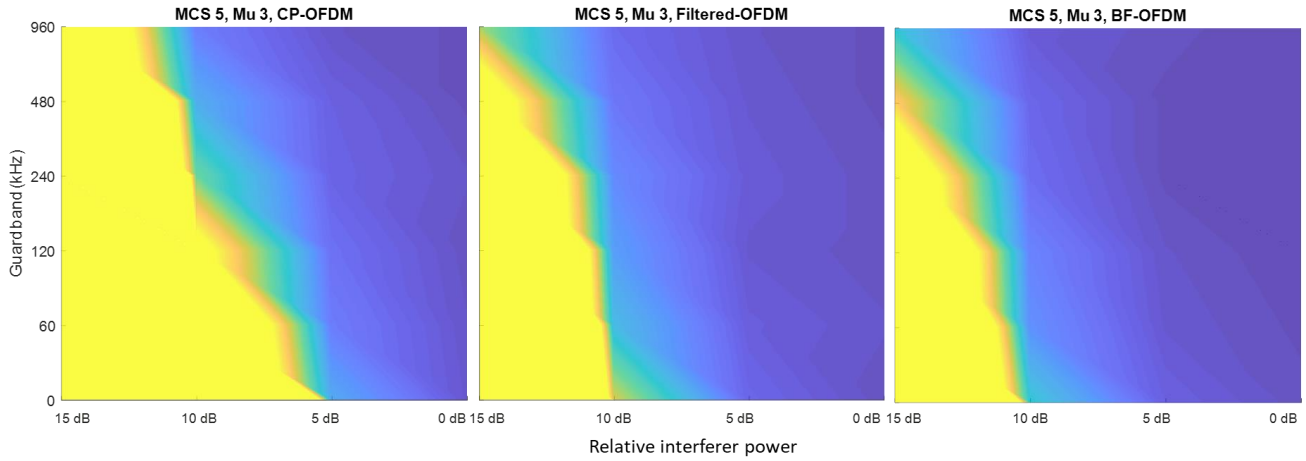

Figure 3-10: PER for MCS 5, μ=3, 15.36 MHz bandwidth. See scale on Figure 3-5.

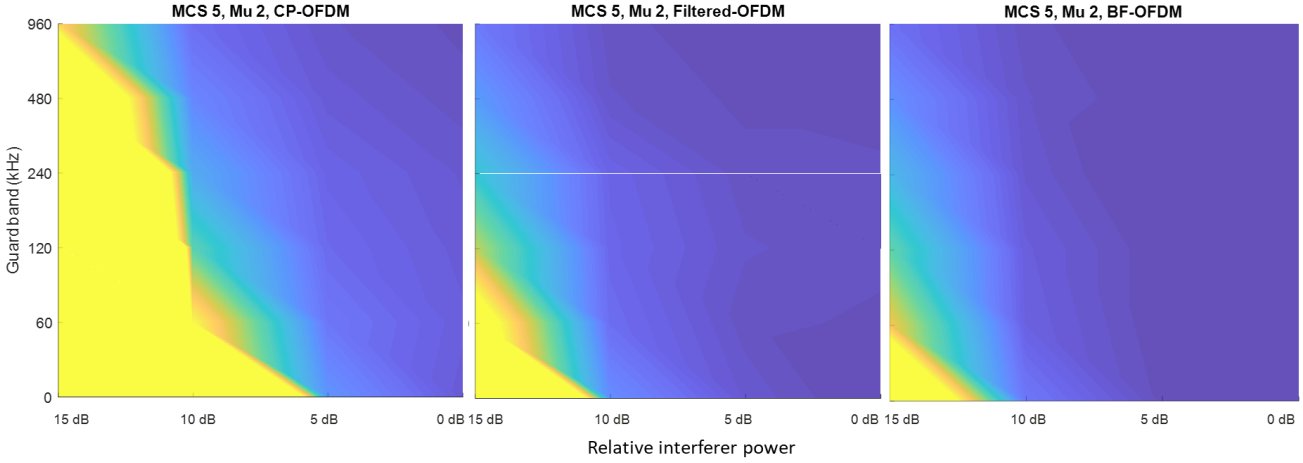

Figure 3-11: PER for MCS 5, μ=2, 15.36 MHz bandwidth. See scale on Figure 3-5.

3.3.2 30.72 MHz bandwidth

Figure 3-12 to Figure 3-17 are for a satellite bandwidth of 30.72 MHz. In this scenario, the throughput loss caused by possible guard bands is given in Table 3-4.

Table 3-4: Throughput loss due to guard bands for the 30.72 MHz bandwidth scenario

Guard band (each side), kHz	Throughput loss, %
0	0.00
60	0.39
120	0.78
240	1.56
480	3.12
960	6.25

For satellite MCS 15, F-OFDM and BF-OFDM perform nearly the same, and improve the performance compared to CP-OFDM. With this latter waveform, a correct PER can be reached only for a low interferer power (<5 dB dB) and with high guard bands (> 240 kHz). By using filtered waveforms, guard bands are no longer necessary, but the interferer power must still be limited (<5 dB). With filtered waveforms, performance is better with numerology 2 than with numerology 3.

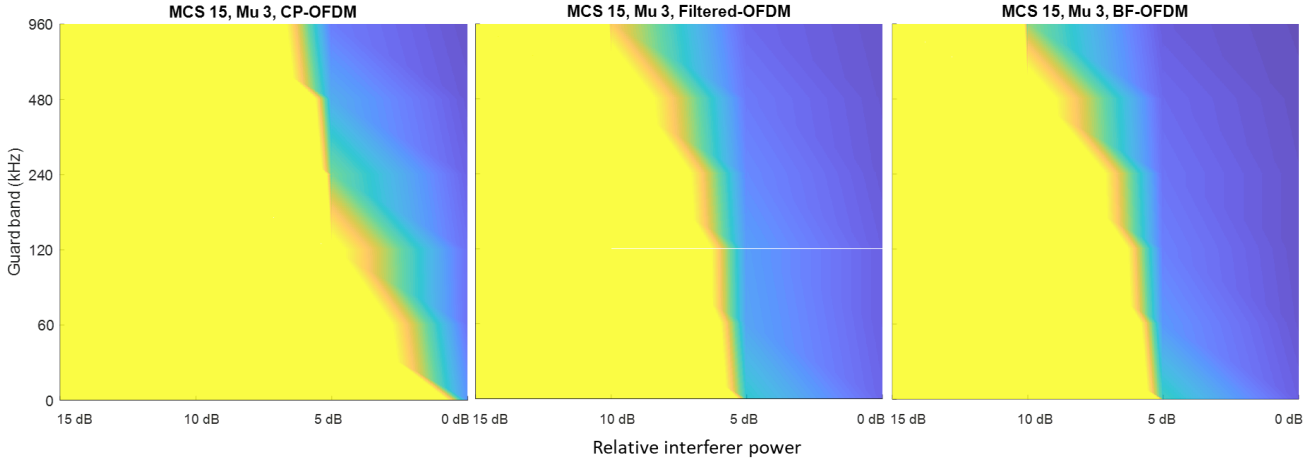

Figure 3-12: PER for MCS 15, μ=3, 30.72 MHz bandwidth. See scale on Figure 3-5.

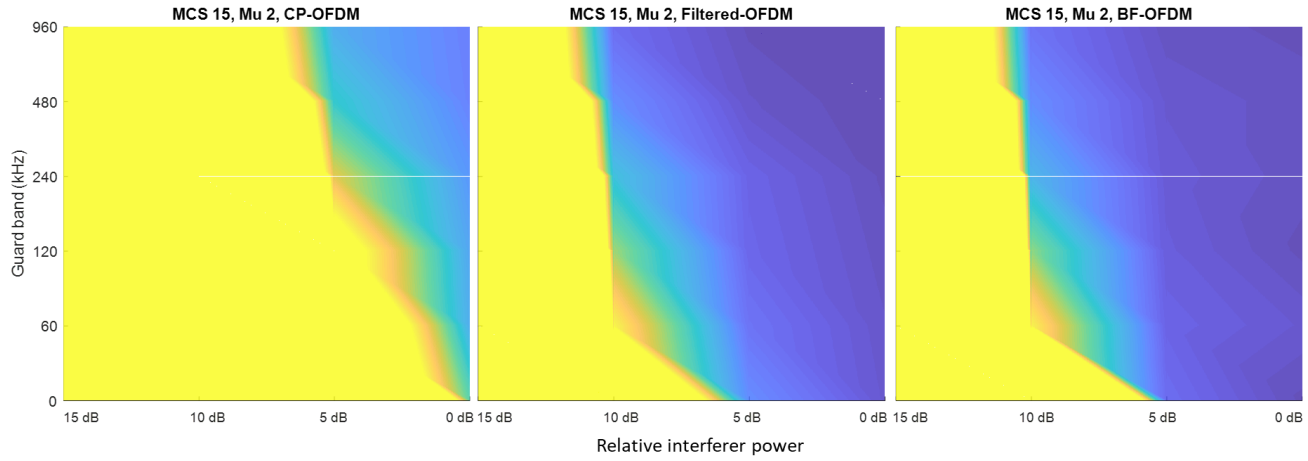

Figure 3-13: PER for MCS 15, μ=2, 30.72 MHz bandwidth. See scale on Figure 3-5.

For satellite MCS 10, BF-OFDM performs a bit better than F-OFDM (specially for numerology 3), and both are more efficient than CP-OFDM. With CP-OFDM, small guard bands are possible only for a very low power interferer (<5 dB). By using BF-OFDM, limited guard bands (120 kHz for numerology 3 and nearly 0 kHz for numerology 2) can be used even for a high power interferer (around 10 dB). Once again, in all the cases, performance is better with numerology 2 than with numerology 3. With numerology 2, very high power interferer (between 10 and 15 dB) can be managed by BF-OFDM, but at the cost of high guard bands (>480 kHz).

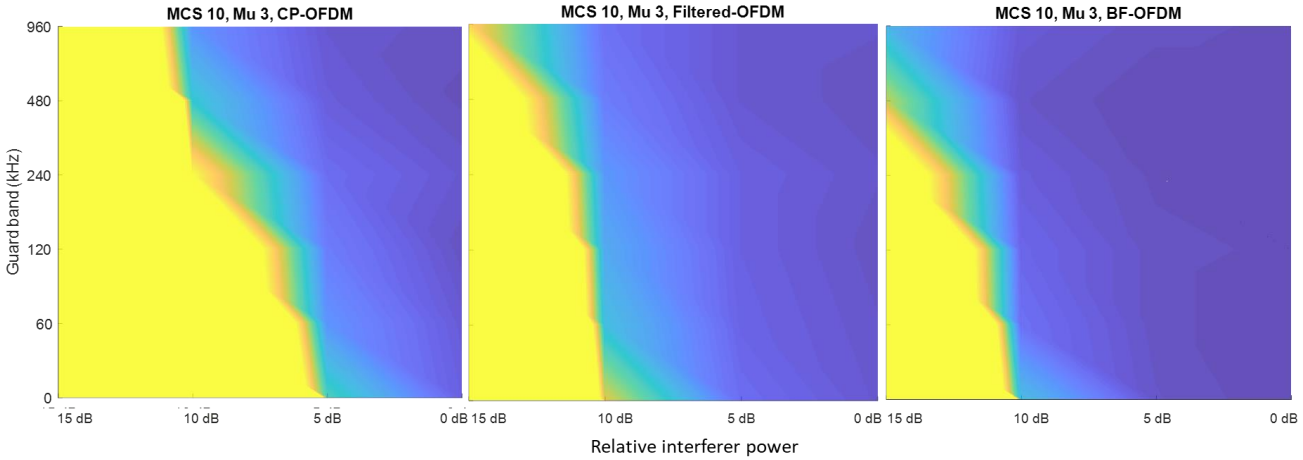

Figure 3-14: PER for MCS 10, μ=3, 30.72 MHz bandwidth. See scale on Figure 3-5.

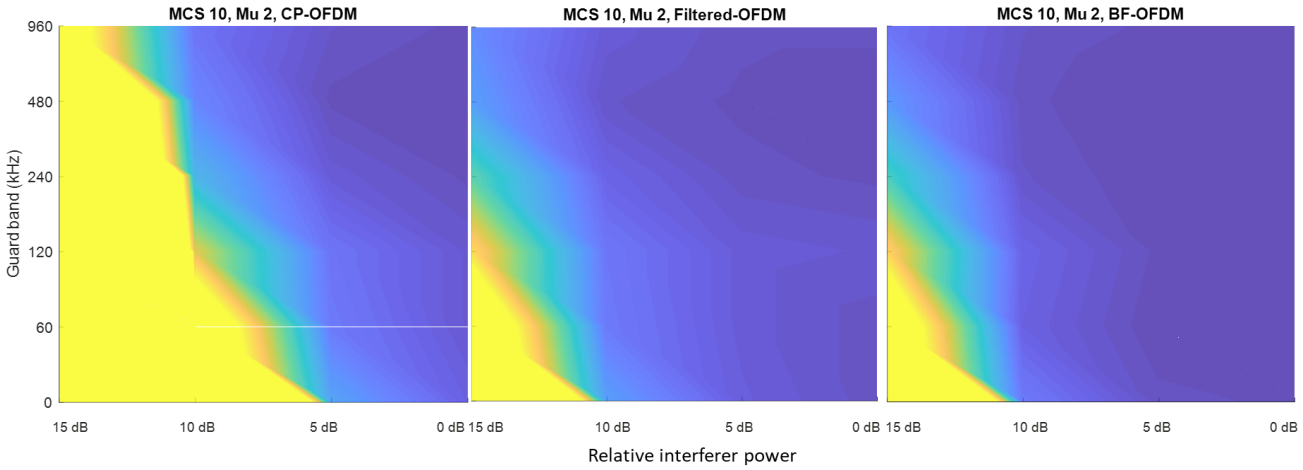

Figure 3-15: PER for MCS 10, μ=2, 30.72 MHz bandwidth. See scale on Figure 3-5.

For satellite MCS 5, the most robust, BF-OFDM performs nearly the same than F-OFDM, and both are much more efficient than CP-OFDM. With CP-OFDM, interferer power up to 10 dB can be managed with guard bands around 240 kHz. By using BF-OFDM, the guard bands can be limited to 120 kHz for numerology 3 and even to nearly 0 kHz for numerology 2.

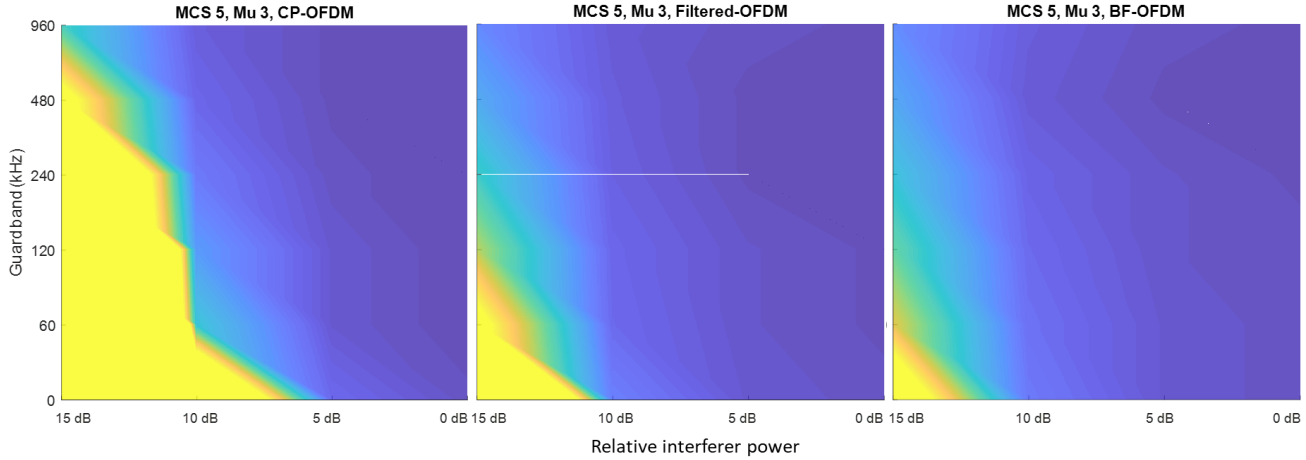

Figure 3-16: PER for MCS 5, μ=3, 30.72 MHz bandwidth. See scale on Figure 3-5.

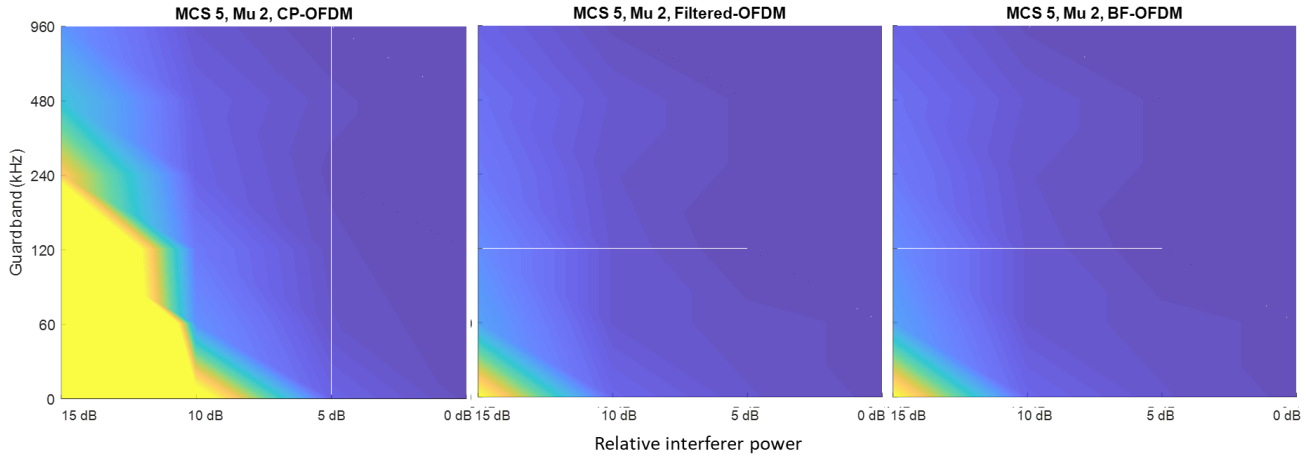

Figure 3-17: PER for MCS 5, μ=2, 30.72 MHz bandwidth. See scale on Figure 3-5.

3.4 Conclusion

We have shown in this study that interference of terrestrial system on frequency adjacent satellite system can be managed by using filtered waveforms. Filtering allows to increase the OoB rejections of the waveform, hence making possible to reduce the frequency guard bands between both systems. F-OFDM and BF-OFDM have comparable performance in this context, but the latter is more suited to the real-time bandwidth reconfigurations that may be required by terrestrial-satellite multi-connectivity.

It must be noted that the OoB rejection capability of a waveform highly depends on the Power Amplifier (PA) response: a badly dimensioned PA causes spectral regrowth and therefore ruins the whole point of using digital filtering techniques. Nevertheless, beyond choosing the appropriate PA (but increasing the cost) or increasing the PA back off (but degrading the link budget), baseband Peak to Average Power Ratio (PAPR) reduction techniques using PA linearization can be efficiently implemented, even with F-OFDM and BF-OFDM [20].

For all these reasons, BF-OFDM has been chosen as the terrestrial waveform to be implemented in hardware (on a FPGA platform) in Work Package 5, for the EU testbed and trial platform.

4 Interference mitigation through RRM

In subsection 4.1, as a means of resource allocation for the cellular base station, an exclusion region design concept is proposed for the cellular base station based on the non-circular-shaped exclusion region. A specific implementation method for realizing the non-circular-shaped exclusion region is also provided. The performance of the proposed exclusion region design scheme is verified by computer simulation.

Subsection 4.2 proposes an overview of candidate interference mitigation mechanisms, all based on RRM coordination, in frequency domains, frequency*time domains or time domains.

In subsection 4.3, an interference mitigation mechanism is selected, amongst several candidates, implemented and evaluated, by means of a RRM simulator, modeling both NTN RAN and terrestrial RANs, interfering each other and connected to the same Core Network. TAS has developed the RRM simulator, implemented one mitigation mechanism and evaluated it across several scenarios with different interferences levels. KPIs have been implemented and operated by post-processing, for performance evaluation purposes.

4.1 Exclusion region design for interference mitigation

4.1.1 Background

Traditionally, a circular-shaped exclusion region was considered for the protection of the satellite Earth station when the satellite and cellular networks coexist in the same frequency band. As seen in Figure 4-1, by allowing the transmission of the cellular base station only at the outside of the circle centered at the satellite Earth station with a certain radius, severe interference experienced by the satellite Earth station can be avoided [21].

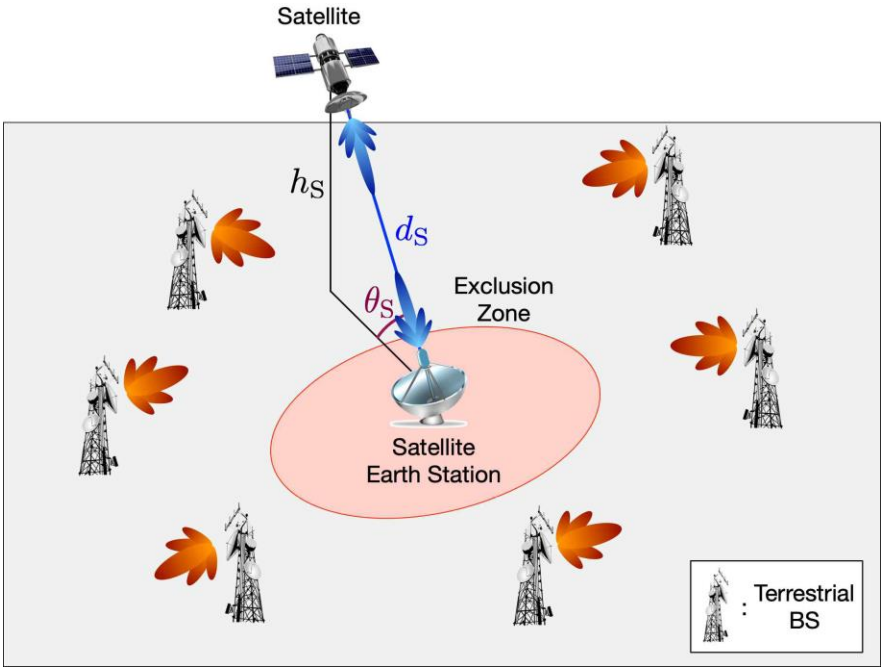

Figure 4-1: A circular-shaped exclusion zone concept

An angular-domain exclusion zone concept was proposed in [22], which utilizes the characteristics of the sector-based transmission at the base station. Since each sector of the base station operates independently, interference to the satellite Earth station can be avoided by turning off a sector covering the cone-shaped coverage area including the satellite Earth station instead of turning off the entire sectors of the base station.

4.1.2 Concept

As discussed above, the circular-shaped exclusion zone is not proper for directional antenna-based transmission. Hence, the above angular-domain exclusion zone concept can be more generalized to design a more efficient exclusion zone. Using the property of the directive antenna, the radius of the exclusion zone can be separately determined along the azimuthal direction. More specifically, the following parameters can be considered whether to turn a specific cellular base station on or off: channel gain, location, and beam direction. If the calculated interference level is less than a preset threshold, it will be okay for the cellular base station to transmit its own signal to the UE. In contrast, if the interference level exceeds the threshold, the cellular base station is required to stop transmission.

The radius of the exclusion zone can be obtained based on statistically allowable exclusion zone radius. For this, it is important to ensure that the average interference from an individual base station is below a certain interference threshold. The radius of exclusion zone towards a specific base station can be obtained from a probabilistic point of view. In other words, the exclusion zone radius from the satellite Earth station is different for each transmit-receive beam gain pair (g_T, g_R).

The instantaneous interference level can be expressed as

$$I_0 = hP_t g_T g_R d^{-\alpha}$$

where h, P_t, d, and α are the channel gain, transmit power, distance, and path loss exponent, respectively. The average instantaneous level is obtained as

$$\begin{aligned} I(d) &= \mathbb{E}_h[I_0 \mid g_T, g_R] \\ &= \mathbb{E}_h[hP_t g_T g_R d^{-\alpha}] \\ &= P_t g_T g_R d^{-\alpha} \end{aligned}$$

Then, the exclusion zone radius can be obtained when the average interference level equals the threshold, as follows:

$$\delta = \left(\frac{\gamma}{P_t g_T g_R}\right)^{1/\alpha}$$

An example of the generated exclusion zone by the proposed exclusion zone design scheme can be illustrated in Figure 4-2. In this example, the exclusion zone radius is determined by the azimuthal directions of the transmit beam of the cellular base station and the receive beam of the satellite Earth station. The receive beam of the satellite Earth station is assumed to be steered to the right direction in the figure. The base station in the orange zone generates its main lobe towards the satellite Earth station, and is located within the main lobe of the receive beam. Hence, its exclusion zone radius needs to be very large. The base station in the blue zone is within the main lobe of the receive beam but its main lobe of the transmit beam is not steered to the satellite Earth station. Thus, its exclusion zone radius is reduced. The base station in the green zone is outside the main lobe of the receive beam but its main lobe of the transmit beam is steered to the satellite Earth station. The base station in the gray zone and the satellite Earth station are steered to the different directions away from each other, allowing a very small exclusion zone radius.

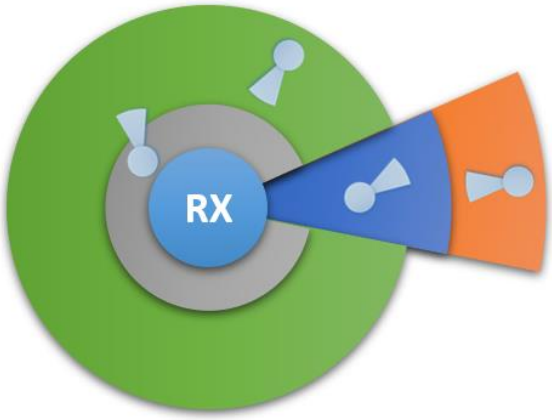

Figure 4-2: Non-circular-shaped exclusion zone example

When compared to the conventional circular-shaped exclusion zone method, the proposed technique can reduce the effect of interference with relatively greater beam gain, given the same number of transmitting base stations.

4.1.3 Algorithm implementation

As illustrated in Figure 4-3, the proposed non-circular-shaped exclusion zone design scheme can be implemented in three steps:

- Step 1: Distribute BSs based on PPP on 2-dimensional space
- Step 2: Specify the transmission limit region & Classify BSs according to beam gain
- Step 3: Remove the BSs in the transmission limit region depending on own beam gain

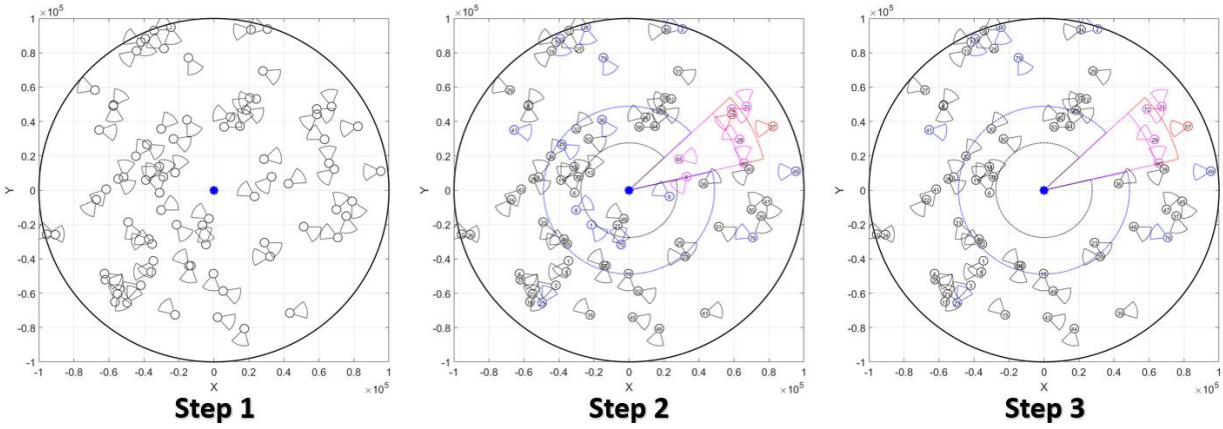

Figure 4-3: Implementation of non-circular-shaped exclusion zone design scheme

4.1.4 Performance

The performance of the proposed algorithm is evaluated via computer simulation. The evaluation metric is success probability which is defined as the probability that the SINR exceeds the threshold. The base stations locations are generated according to the Poisson point process. The detailed simulation parameters are summarized in Table 4-1

Table 4-1: Simulation parameters

Parameter	Value
Distance between Satellite Station and Satellite Earth Station	$4 \times 10^3 \mathrm{km}$
Radius of Exclusion Zone	$1\ \mathrm{km}$

Interference Threshold	2.56×10^{-7}
Transmit Power of Satellite	20Watt
Power of the cellular BS	20Watt
Beam-width of the satellite and the satellite earth station	10°
Beam-width of the cellular BS	30°
Antenna side-lobe gain of the satellite earth station	-10dBi
Antenna main-lobe gain of the BS	1dBi
Noise figure	−172.6dBm
Bandwidth	10^7Hz

For fairness in all performance comparisons, the number of removed (i.e., non-transmitting) base stations is set to be equal for the same area. Figure 4-4 shows the performance of the proposed scheme compared with the conventional scheme, i.e., a circular-shaped exclusion region. It is seen that the proportion of the successful decoding is improved by the proposed scheme using interference threshold-based exclusion radius determination.

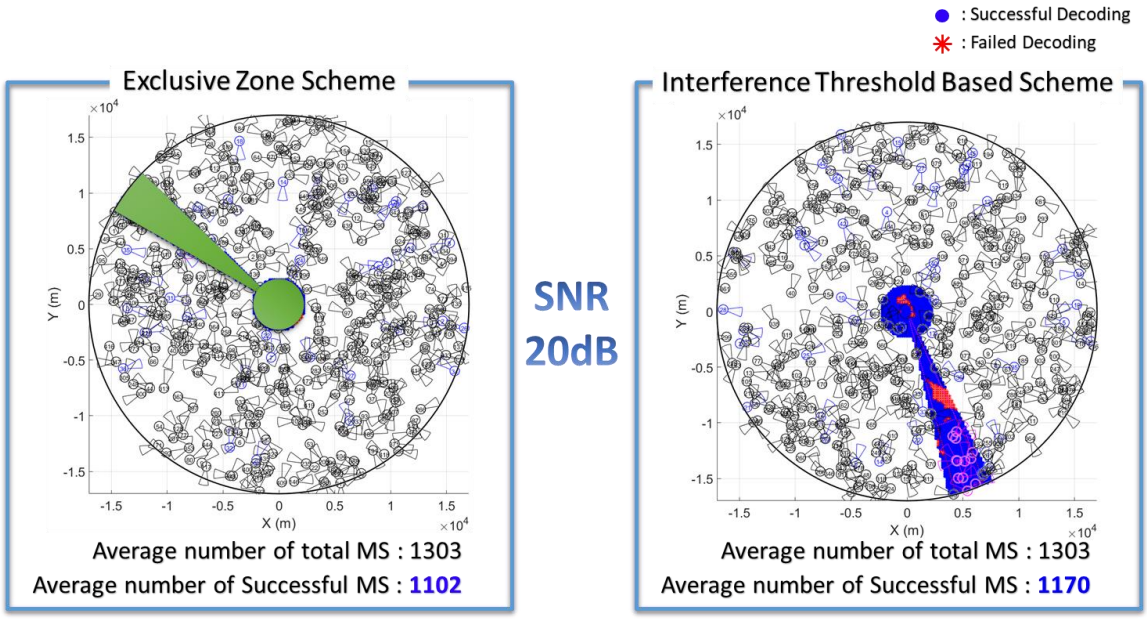

Figure 4-4: Performance comparison with the conventional scheme

The success probability as a function of the number of removed base stations is depicted in Figure 4-5. It is seen that the proposed technique based on interference threshold has significantly higher success probability than the exclusive zone-based scheme.

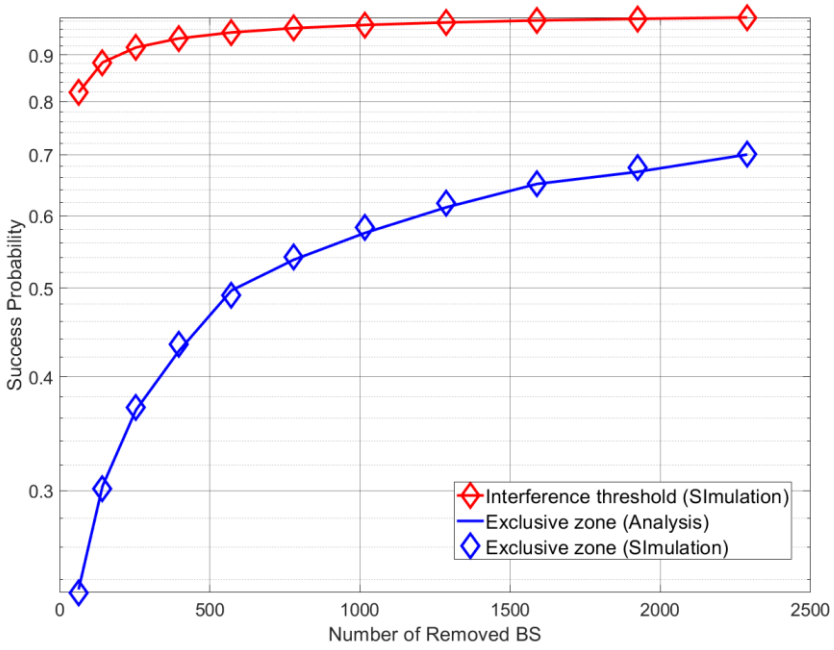

Figure 4-5: Success probability vs. Number of removed base stations

4.1.5 Conclusion

In this subsection, a non-circular-shaped exclusion zone design scheme was proposed, which utilizes the effect of transmit/receive beam directions on the interference level at the satellite Earth station. Cellular base stations incurring high interference are removed (i.e., turned off) by designating a larger exclusion zone radius. Simulation results revealed that the proposed scheme outperforms the conventional circular-shaped exclusion zone design in terms of the success probability of satellite network and the performance of coverage area in the cellular network.

4.2 Coordinated RRM schemes

The objective of this chapter is to give an overview of the candidate RRM coordination schemes, for an implementation in a RRM simulator, NS-3 based platform and extended to face NTN links constraints.

Table 4-2: RRM coordination schemes overview

RRM coordination schemes	Short description	Discussion and decision
Frequency domain		
Full Frequency Reuse (FFR)	No frequency band partitioning. One region type, FRF = 1, 1 unique sub-band for all cells. Sat / cells Power coordination in the frequency domain. High Interference levels from neighboring cells and from / towards SSA, if use of the same frequency. Lower level if	**Pro**: Simple. **Cons**: Not a RRM coordination scheme. It is typically a non-coordination case. It could be used to benchmark other coordination scheme. **Decision**: Not implemented.

RRM coordination schemes	Short description	Discussion and decision
	neighbored frequency are used. Satellite PFD limits are required, for terrestrial isolation purposes. See Figure 4-6.	
Hard Frequency Reuse (HFR) with FRF=5 per disjoint cluster basis	Frequency BW partitioning into 5 disjoint bands, assigned to clusters (cells) that are not in the same neighborhood (cells): 5 region types, FRF = 5: • 1 unique sub-band for SSA • 1 unique sub-band per clusters. Cells Power coordination within a cluster, in the frequency domain. See Figure 4-7.	**Pro**: Reduced ICI between cells and cells of neighbored clusters. Reduced ICI from / towards SSA. However, Satellite PFD limits are required. Peak Data Rate is reduced by the Reuse factor FRF. But the FRF is lower than in scheme HFR. **Cons**: Band consuming as FRF is > 1. **Decision**: A simple version could be implemented in NS-3 platform. The Power Control is partially implemented and the resource are partitioned per RBG basis. The colorization pattern should be revisited, to avoid neighbored terrestrial cells with the same color. One color should be assigned to the NTN cell.
Strict Frequency Reuse with FRF=5, per disjoint cluster basis	Frequency band partitioning into 5 disjoint bands (FRF-5), for coordination between clusters and between clusters and SSA: One common sub-band of the system bandwidth is used in each cell interior (FRF-1), while the other part of the bandwidth is divided among the neighboring eNBs and the SSA, as in hard frequency reuse (FRF = 4 for cells + 1 for SSA) Cells coordination within a cluster (such as beam forming, power reduction, ICIC / eICIC, load balancing). See Figure 4-8.	**Pro**: Reduced ICI between cells and cells of neighbored clusters. Reduced ICI from / towards SSA. However, Satellite PFD limits are required. Peak Data Rate is reduced by the FRF factor. But FRF is lower than in scheme StFR-1. **Cons**: A sub-band is dedicated to satellite. This strict FR is not specifically tuned for satellite coverture, but for terrestrial cells. **Decision**: Too complex. Not

RRM coordination schemes	Short description	Discussion and decision
		specific to NTN cell. Not implemented.
Soft Frequency Reuse v1 scheme for cells, per cluster basis and Hard frequency reuse for SSA (FRF=2)	Frequency band partitioning into 2 disjoint bands (FRF-2), for coordination between terrestrial clusters and (terrestrial cluster and SSA): • Each gNB transmits over the entire system bandwidth (yellow) • The SSA transmit in its own sub-band (brown) • In each cluster, there are two sub-bands and regions, within UEs are served with different power levels. In Soft Frequency Reuse v1: ▪ One sub-band / region is dedicated to the terrestrial cell-edge UE. It may also be used by the terrestrial cell center UE but with reduced power level and only if it is not occupied by the cell-edge UE. ▪ The Cell-center sub-band / region is available to the cell-center UE only. Within a terrestrial cluster, other RRM coordination schemes may be applied, such as beam forming, power reduction, ICIC / eICIC. See Figure 4-9.	**Pro**: Reduced ICI between cells and cells of neighbored clusters. Reduced ICI from / towards SSA. However, Satellite PFD limits are required. Peak Data Rate is enhanced, by the FRF factor, which is low. **Cons**: A sub-band is dedicated to satellite. This strict FR is not specifically tuned for satellite coverture, but for terrestrial cells. **Decision**: Too complex. Not specific to NTN cell. Not implemented.
Frequency*Time domains		
ICIC (Inter-Cell Interference Coordination)	Cells use their own band and the entire bandwidth (yellow) and a dedicated sub-band per cluster, in the interference areas. The SSA has to share the entire band with the cells, in time sharing (brown). A specific cluster Cs is assigned to SSA Each cell cluster Ci, makes use of: - Dedicated UL PRBs for the Cell Center UE - Dedicated UL PRBs for the Cell Edge UE Terrestrial gNB of cluster Ci:	**Pro**: It has similarities with Hard Frequency Reuse (HFR), but it better suits the T3.4 working assumption: spectrum sharing between NTN et terrestrial RANs. Few band consuming as FRF =1. It is in the time domain also because 1ms PRB have to be scheduled by gNB, in a coordinated way. **Cons**: Not foreseen any “conservative”.

RRM coordination schemes	Short description	Discussion and decision
	- Detects interference with cluster Cs, on Ci UL PRBs 1 and - Keeps scheduling on Ci UL PRBs 2 of cell edge UEs. The Satellite gNB cluster: - Schedules Reduced Power on Ci UL PRBs 1 and does not schedule on Ci UL PRBs 2 for of cell edge UEs. See Figure 4-10.	**Decision**: Can be implemented on a platform modeling PRBs, such as NS-3. The detection of interference can be simplified by provisioning radio resource allocation per cluster basis, managed a network controller entity.
Frequency domain: Intra or Inter-band		
CA based Cross-carrier scheduling based ICIC: intra-band case	Cells operate their own band, the entire bandwidth (yellow) and a dedicated sub-band per cluster, in the interference areas. The SSA has to share the entire band with the cells, in time sharing (brown). Cellular gNB: - Uses fi CC as PCC. Cell edge UEs are scheduled on PCC. - Uses fs CC and fj CC (j <> i) as SCCs. Cell edge UEs are not scheduled on SCCs. - AND/OR Manages Zero Power (ZP) or Reduced Power (RP) on the SCC. NTN gNB: - Uses fs CC as PCC - Uses fi CC as SCC. Cell edge UEs on SCC are not scheduled on SCC. - Increases scheduled power on PCC compared to the SCCs. See Figure 4-12.	**Pro**: Complies with the working assumptions: spectrum sharing. **Cons**: Not native in NS-3 but may be simulated by provisioning OFDM sub-carriers per cluster basis. **Decision**: Candidate for a further implementation and performance evaluation. Can be implemented on a platform modeling Sub-carriers and PRBs, such as NS-3. The PCC and SCC should be provisioned per cluster basis, by a network controller entity.
Time domain		
eICIC (Inter-Cell Interference Coordination) (FRF=1)	Cells use their own band and the entire bandwidth (yellow) and a dedicated sub-band per cluster, in the interference areas. The SSA has to share the entire band with the cells, in time sharing (brown). Each cell cluster Ci makes use of:	**Pro**: Complies with the spectrum sharing working assumptions. **Cons**: Complex to implement. Requires a deep MAC layer scheduling change to comply with the ABS (Almost Blank Sub-Frames) scheduling, which

RRM coordination schemes	Short description	Discussion and decision
	- Ci DL PRBs for the Cell Center UE - Ci DL PRBs for the Cell edge UE Cluster Ci gNBs: - Detects interference on Ci DL sub-frames 1,2,3 and - Schedules cell center UE on Ci DL sub-frames 4,5 Satellite gNB: - Decreases / Zero power on DL sub-frames 1,2,3 and - Does not schedule SSA UEs on DL sub-frames 4,5 See Figure 4-11.	is complex and not available natively in NS-3. **Decision**: Too complex. Not implemented.

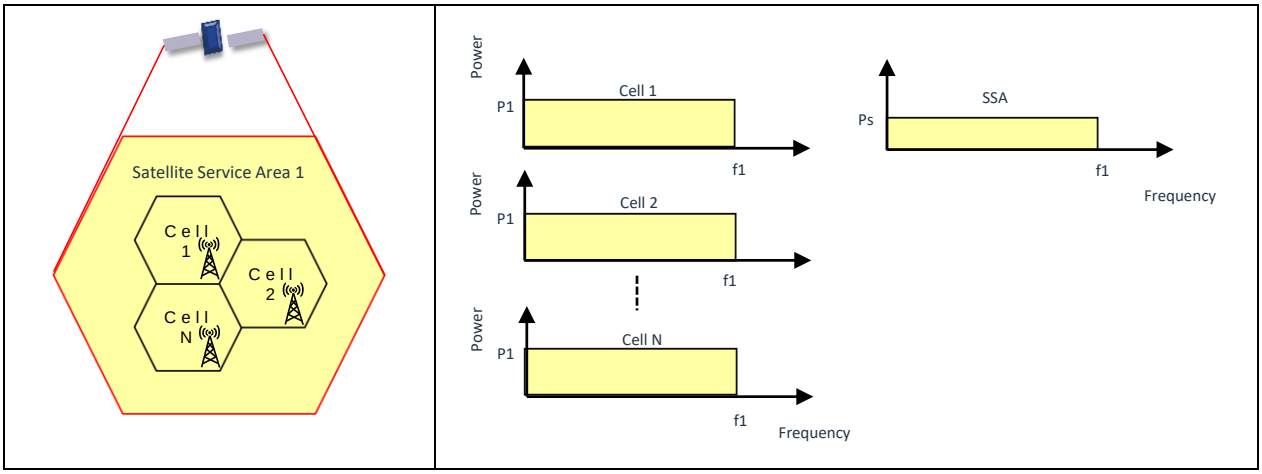

Figure 4-6: Full Frequency Reuse (FRF=1)

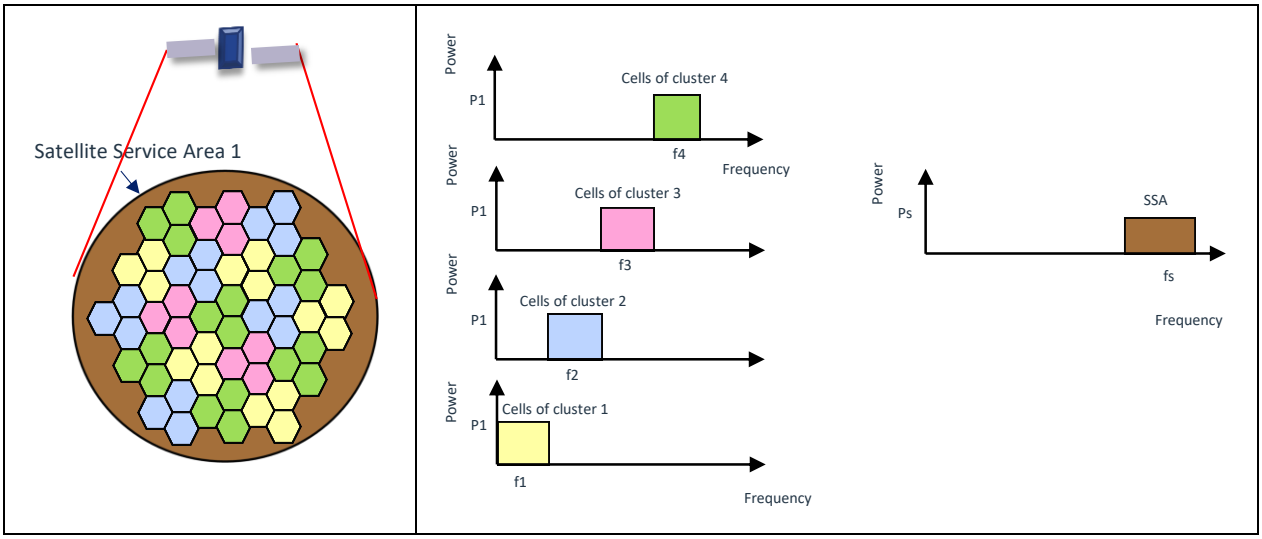

Figure 4-7: Hard Frequency Reuse (FRF=5)

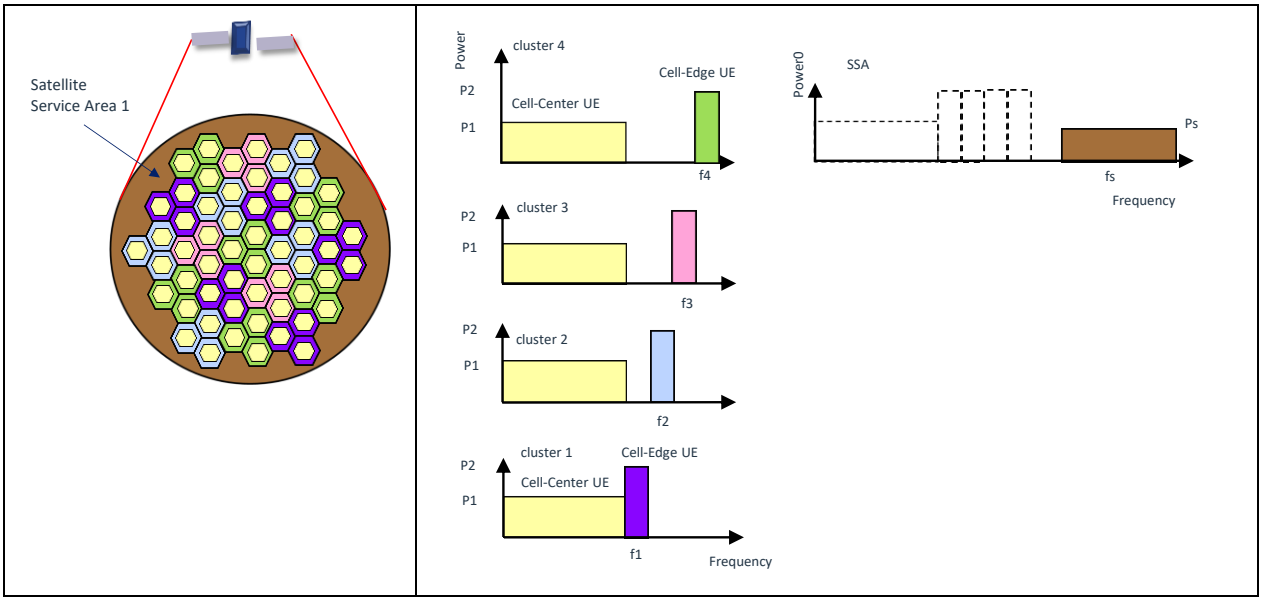

Figure 4-8: Strict Frequency Reuse (FRF=5)

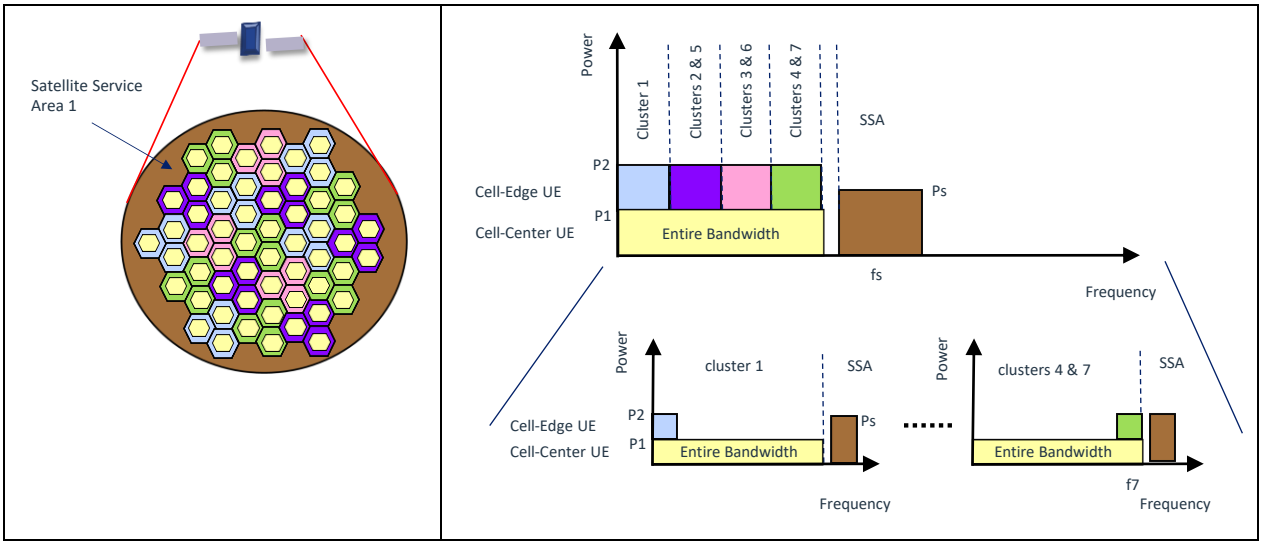

Figure 4-9: Soft Frequency Reuse v1 scheme for cells, per cluster basis

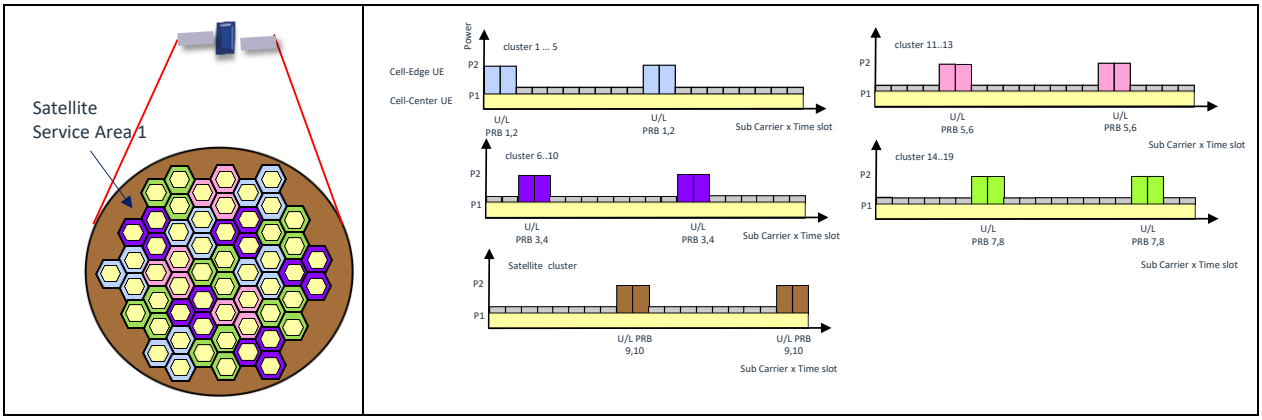

Figure 4-10: ICIC (Inter-Cell Interference Coordination)

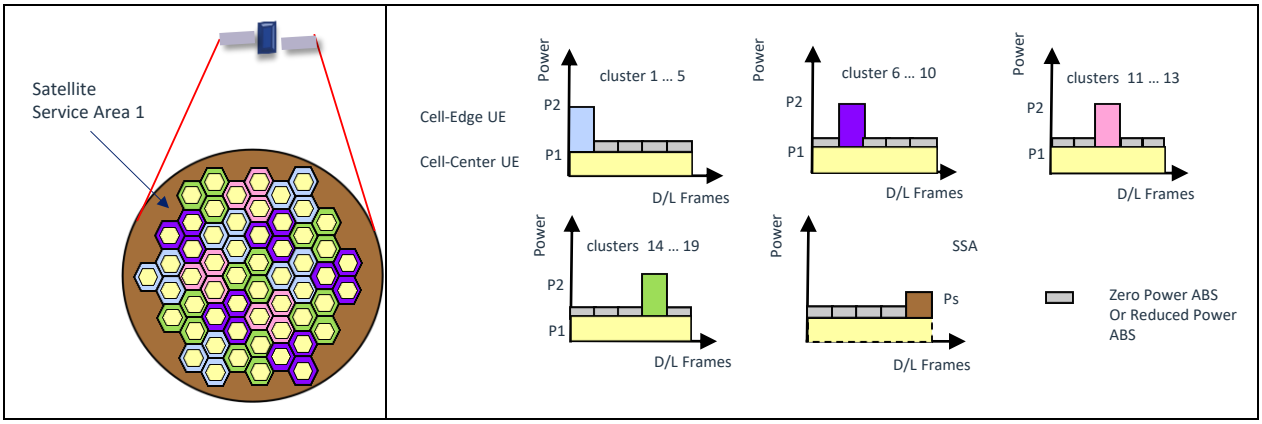

Figure 4-11: eICIC (Inter-Cell Interference Coordination)

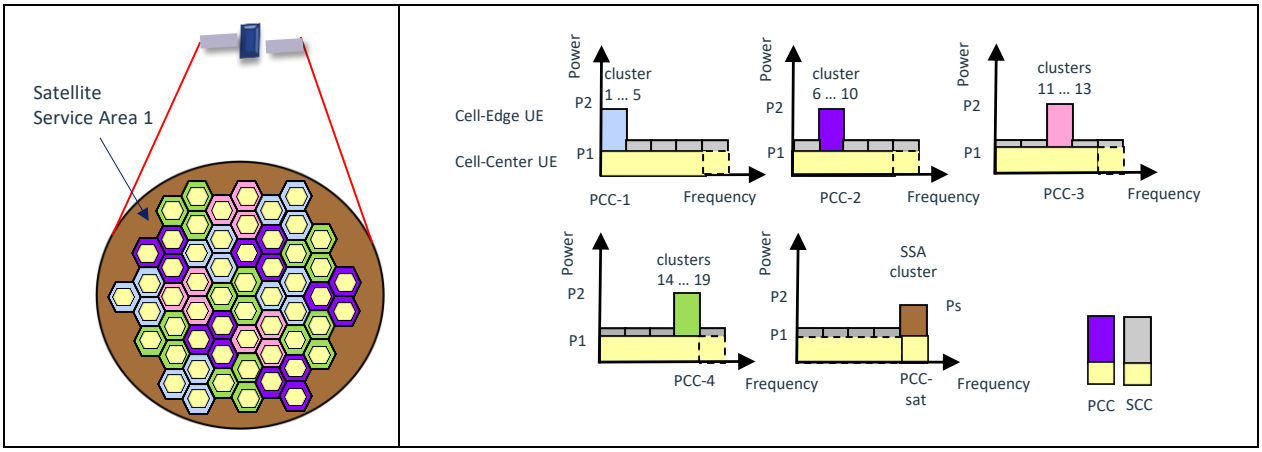

Figure 4-12: CA based Cross-carrier scheduling based ICIC (intra-band case)

4.3 Performance evaluation of a RRM colorization scheme, based on simulations

4.3.1 Interferences modeling

The simulations are based on the following assumptions:

- The radio user links are modeled, not the feeder link.
- The NTN UE – served by the NTN base station - are co-located with their peer terrestrial UE, served by their terrestrial base station.
- The NTN and terrestrial base stations transmits on the same DL frequency band.
- The NTN and terrestrial UE transmits on the same UL frequency band.
- As the FDD mode is operated, the DL frequency and the UL one are separated and we consider they don't interfere each other. That may be too optimistic in a real system, whenever these frequency bands are adjacent.
- As the objective if this study is to evaluate an interference mitigation mechanism between NTN and terrestrial RAN, and not between terrestrial RAN, a resource colorization scheme / pattern is applied to terrestrial base stations to avoid interfering each other and skew the performance evaluation of the mechanism of interest.

As depicted in Figure 4-13 and Figure 4-14, the following interferences have been modeled, in the simulator:

- Interferences on the signal received by terrestrial entities:
    - The terrestrial UE are the receivers and potential victims of the satellite aggressor (on-board NTN base station on-board RRU), in the DL frequency band
    - The terrestrial base stations are the receivers and potential victims of NTN UE aggressors, in the UL frequency band
- Interferences on the signal received by NTN entities:
    - The NTN UE are the receivers and potential victims of the terrestrial base stations, in the DL frequency band
    - The satellite (on-board NTN base station or RRU) is the receiver and potential victim of the terrestrial UE, in the UL frequency band

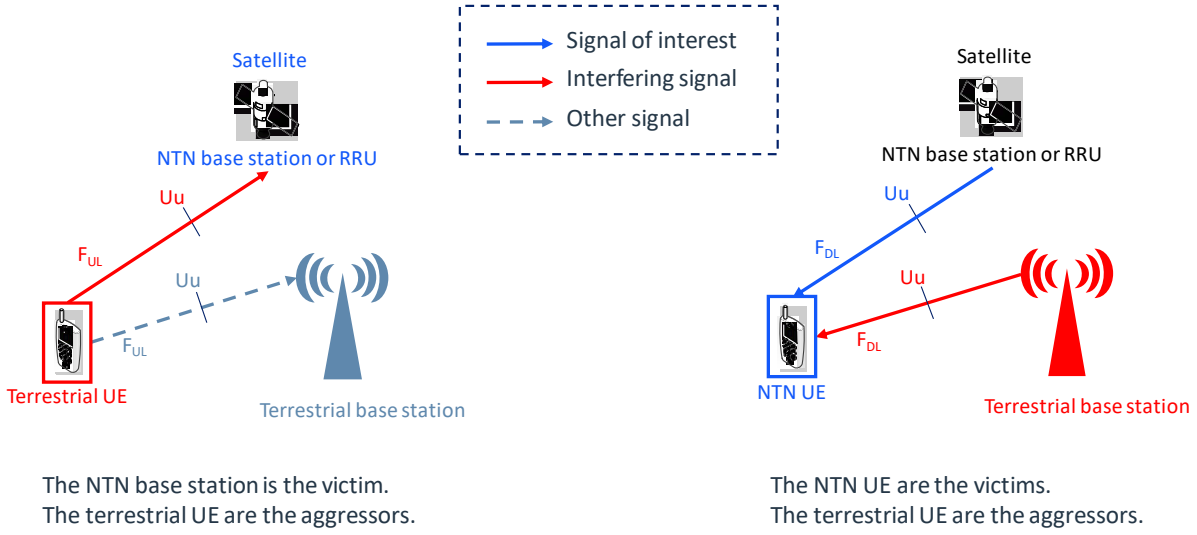

Figure 4-13: Potential victim NTN entities

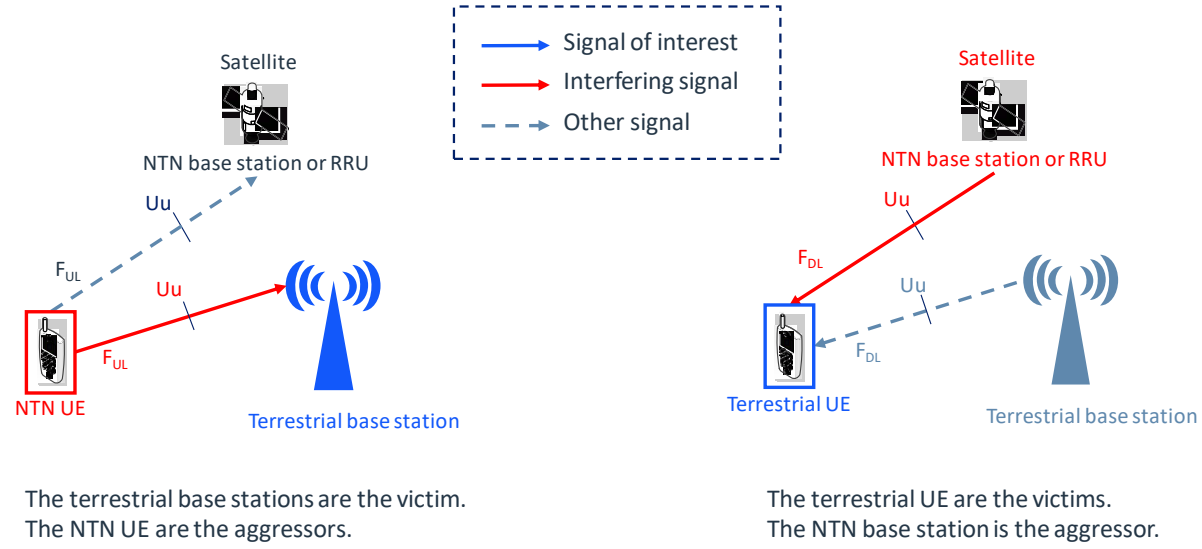

Figure 4-14: Potential victim terrestrial entities

4.3.2 Qualitative analysis

For the qualitative approach, in this case, SINR heat maps have been generated and are compared each other over several scenarios:

- no overlapping between NTN and terrestrial RANs, as RRM coordination scheme is applied,
- 80% overlapping ratios (no coordination and high interference level).
- Whatever the overlapping ratio, the elevation angle of the NTN cell center is 90°, for this study. Other elevation angles may be handled, provided other simulation runs and results post-processing.

A heat map is a thermal equivalent map, where the high interference spots are mapped to "cold" color (blue) and low interference spots, are associated to "hot" color (yellow), with a decreasing pallet.
Two heat map types have been generated, by post-processing:

- Heat maps of SINR received by the terrestrial UE (DL direction only)
  - The terrestrial UE receivers are victims of the satellite (on board NTN base station or RRU), in the DL frequency band
- Heat maps of SINR received by the NTN UE (DL direction only)
  - The NTN UE receivers are victims of the terrestrial base stations, in the DL frequency band

There is no way for modeling the heat maps in the UL direction.

4.3.2.1 Terrestrial DL SINR case

The generated heat maps for terrestrial UE are depicted in .
The triangles depict terrestrial base stations and the points figure terrestrial UE.

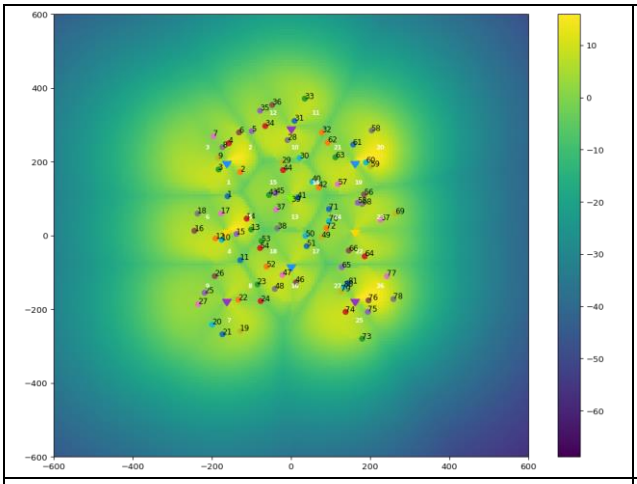

Figure 4-15: SINR Heat maps of terrestrial UE – 90° elevation, no resource (PRB) overlapping

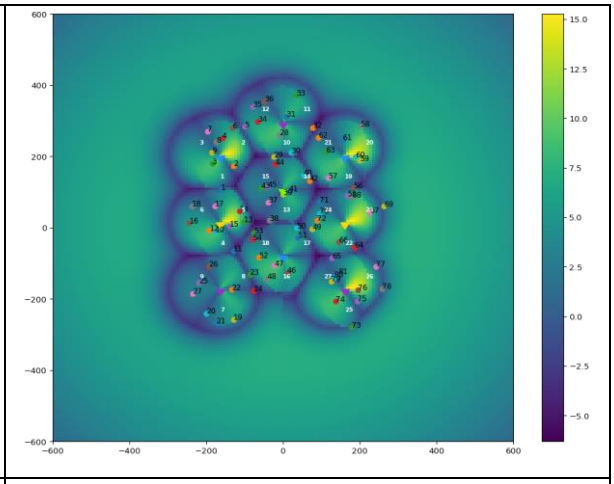

Figure 4-16: SINR Heat maps of terrestrial UE – 90° elevation, 80% resource (PRB) overlapping ratio

For the terrestrial UE case, the trend analysis shows that:

- With a high resource overlapping ratio (right figure) between NTN and terrestrial RANs, the signals received by the terrestrial UE are interfered by the satellite, especially at the terrestrial cells edges, where the terrestrial signals strength decrease. "Cold" colors are globally dominant in the studied area.
- Without any resource overlapping ratio (left figure), the signals received by terrestrial UE are strong. "Yellow" colors are globally dominant in the studied area. The signals are weaker at the terrestrial cell edges, due to terrestrial base station antenna diagram.

4.3.2.2 NTN DL SINR case

The generated heat maps for NTN UE are depicted below.
The triangles depict terrestrial base stations and the points figure NTN UE.

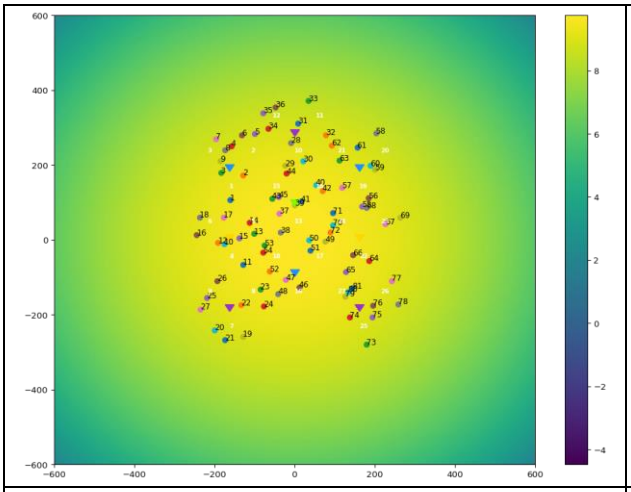

Figure 4-17: SINR Heat maps of NTN UE – 90° elevation, no resource (PRB) overlapping

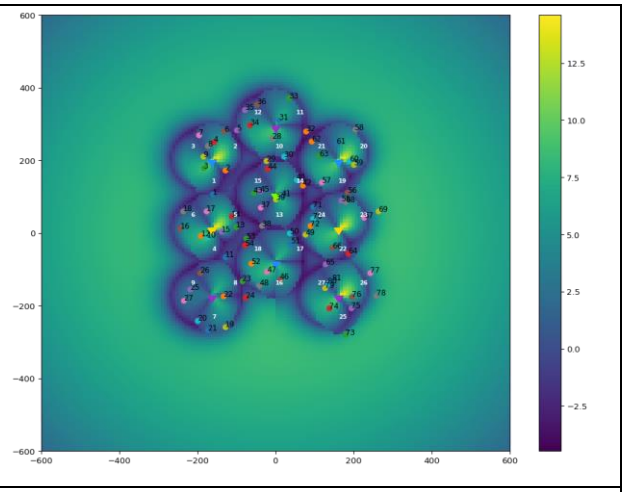

Figure 4-18: SINR Heat maps of NTN UE – 90° elevation, 80% resource (PRB) overlapping ratio

For the NTN UE case, the trend analysis shows that:

- With a high resource overlapping ratio (right figure) between NTN and terrestrial RANs, the signals received by the NTN UE are interfered by the terrestrial base stations. “Cold” colors are globally dominant in the studied area.
- Without any resource overlapping ratio (left figure), the signals received by the NTN UE are strong. “Yellow” colors are globally dominant in the studied area.

4.3.3 Quantitative analysis

4.3.3.1 NTN DL SINR case

For the quantitative approach, in this case, median SINR values the CDF SINR are used and compared over several scenarios: no overlapping between NTN and terrestrial RANs, as RRM coordination scheme is applied, 40% overlapping ratio (no coordination and intermediate interference level), 80% overlapping ratios (no coordination and high interference level).
The Figure 4-19 shows how the UE are positioned by simulation, at different distances (meter) from the satellite. As expected, the distance increases when the elevation angle decreases and reciprocally.
The elevation angle of the NTN cell center is 90° elevation angle, for this study.
Other elevation angles may be handled, provided other simulation runs and results post-processing.

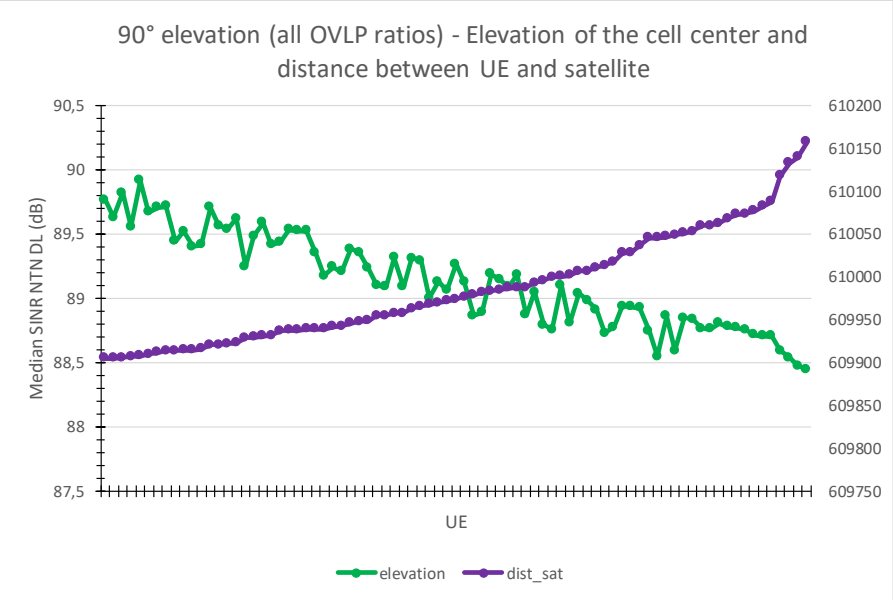

Figure 4-19: UE positioning by simulation

For RRM coordination scheme performance evaluation and trend analysis purposes, three NTN SINR DL median curves per overlapping ratio basis, have been reported on the same Figure 4-20:

- The median curve (in blue) for the lowest simulated overlapping ratio (0% OVLP) matches the lowest interferences level.
- The median curve (in orange) for the intermediate simulated overlapping ratio case (40% OVLP) matches an intermediate interferences level
- The median curve (in grey) for the worst simulated overlapping ratio case (80% OVLP) matches the highest interferences level

The UE are sorted by increasing distance from the satellite, from the left to the right of the X-axis.

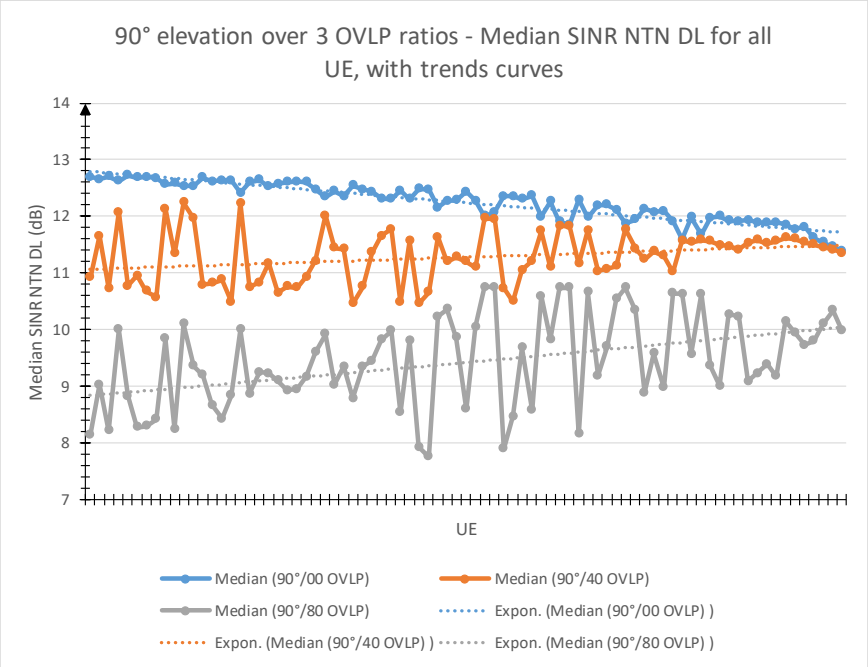

Figure 4-20: NTN SINR DL median curves

To evaluate more accurately the impact of the RRM coordination scheme to mitigate interferences, further curves are shown in Figure 4-21. These curves depict the measured difference between:

- the median SINRs with the 0% overlapping ratio and the median SINRs with the highest tested overlapping ratio (80%), per UE basis and
- the median SINRs with the 0% overlapping ratio and the median SINRs with an intermediate overlapping ratio (40%), per UE basis

The trend analysis shows that the difference (therefore, the benefit) is very high for the UE closer to the satellite and quite still comfortable for the UE which are more distant:

1. Median SINR values differences between low and high overlapping ratios are in the range [0.9dB; 4.8dB]
2. Median SINR values differences between low and high intermediate overlapping ratios are in the range [0dB; 2.2dB]

For the case 2 above and for few UE (up to 5 UE), the benefit of the interference mitigation is not demonstrated, because their SINRs have quite the same value.

In regards of these median SINR curves, the efficiency of the simulated RRM coordination scheme seems to be globally efficient, as it mitigates interferences, whatever the distance of the UE from the satellite.

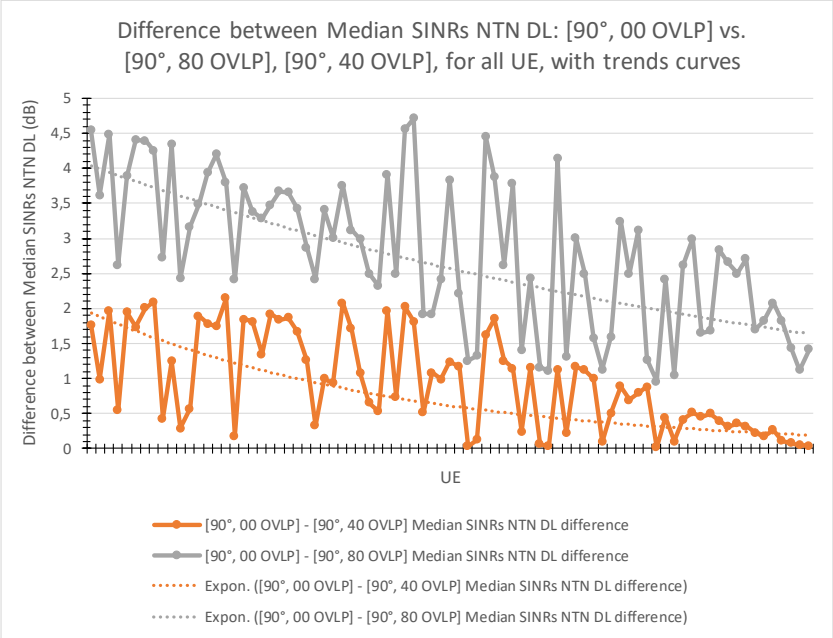

Figure 4-21: Difference between NTN DL SINR curves across different overlapping ratios

In the following, the SINR distribution is analysed for selected UEs only.
SINR DL CDFs of three NTN UE are depicted in Figure 4-22, Figure 4-23 and Figure 4-24 according to:

- UE54 is closer to the satellite than UE61 and UE61.
- UE61 is more distant from the satellite than UE54 and UE79.
- UE79 is at an intermediate distance from the satellite, in regards of UE54 and UE61.

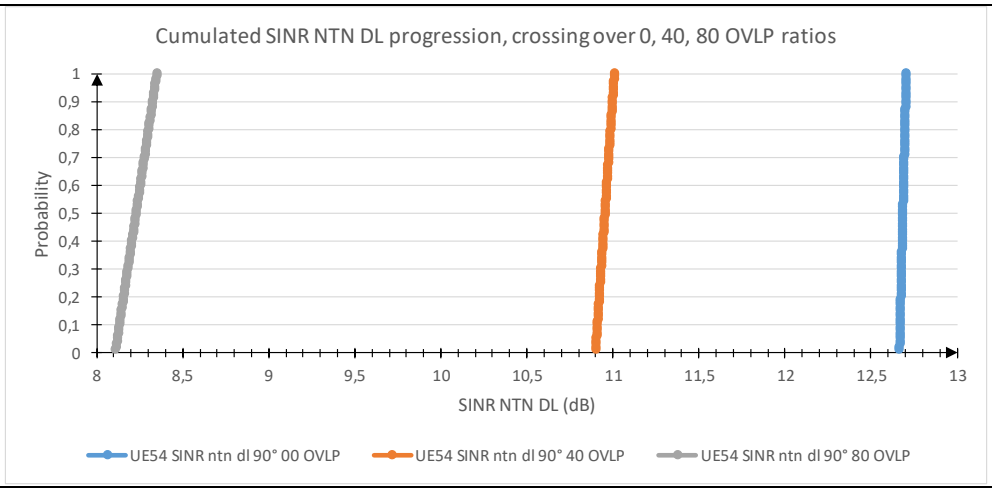

Figure 4-22: NTN UE54 – 90° - SINR DL Trend analysis across different overlapping ratios

For the closer UE to the satellite (UE54), in regards of median SINR value (for CDF = 0.5):

- The difference between SINR/0 OVLP ratio (no overlapping and lowest interferences level) and SINR/80 OVLP ratio (worst simulated overlapping ratio and highest interferences level) is approximately 11.7 dB – 8.25 dB = 3.45 dB while
- The difference between SINR/0 OVLP ratio and SINR/40 OVLP ratio (intermediate overlapping ratio and intermediate interferences level) is approximately 11.7 dB – 11.0 = 0.7 dB

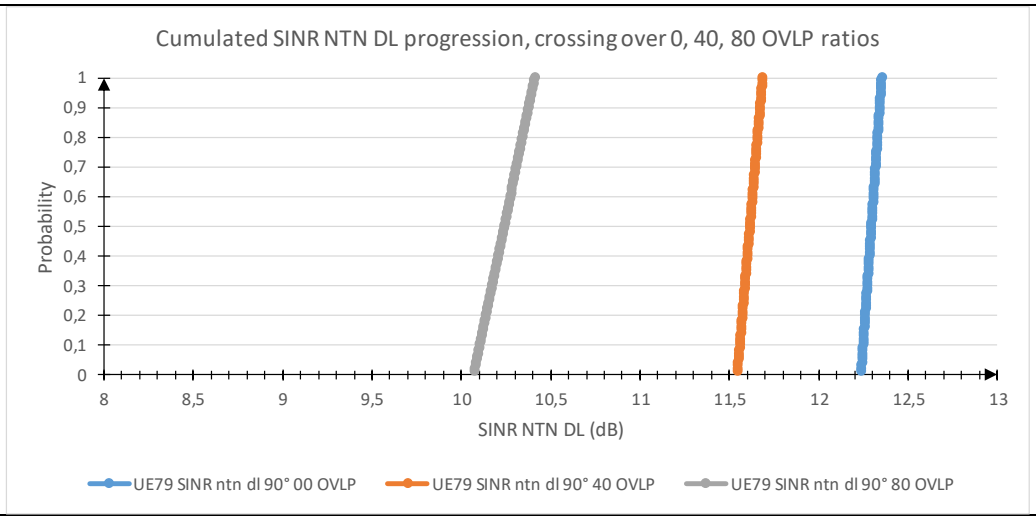

Figure 4-23: NTN UE79 – 90° - SINR DL Trend analysis across different overlapping ratios

For the UE at intermediate distance from the satellite (UE79), in regards of median SINR value (for CDF = 0.5):

- The difference between SINR/0 OVLP ratio (no overlapping and lowest interferences level) and SINR/80 OVLP ratio (worst simulated overlapping ratio and highest interferences level) is approximately 12.3 dB – 10.25 dB = 2.05 dB while
- The difference between SINR/0 OVLP ratio and SINR/40 OVLP ratio (intermediate overlapping ratio and intermediate interferences level) is approximately 12.3 dB – 10.2 = 2.1 dB

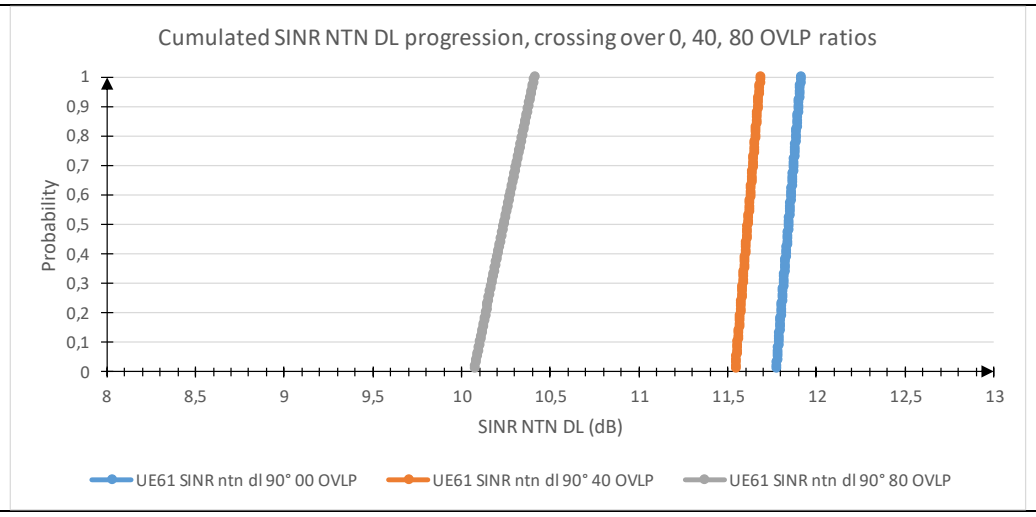

Figure 4-24: NTN UE61 – 90° - SINR DL Trend analysis across different overlapping ratios

For the more distant UE from the satellite (UE61), in regards of median SINR value (for CDF = 0.5):

- The difference between SINR/0 OVLP ratio (no overlapping and lowest interferences level) and SINR/80 OVLP ratio (worst simulated overlapping ratio and highest interferences level) is approximately 11.85 dB – 10.2 dB = 1.65 dB while
- The difference between SINR/0 OVLP and SINR/40 OVLP (intermediate overlapping ratio and intermediate interferences level) is approximately 11.85 dB – 11.6 = 0.25 dB

The trend analysis shows that the closer the distance between UE and satellite, the higher the difference between the SINRs across different per overlapping ratio.

4.3.3.2 NTN UL SINR case

As for the previous case, for RRM coordination scheme performance evaluation and trend analysis purposes, three NTN SINR UL median curves per overlapping ratio basis, have been reported on the same Figure 4-25:

- Regarding the median curve (in blue) for the lowest simulated overlapping ratio (0%):
  - The SINR UL median values are globally homogeneous and decrease while the distance to the satellite increases,
  - Except for first NTN UE transmitters, closer to the satellite: their SINR received at satellite side, is very high.
  - The terrestrial UE co-located to NTN UE do not interfere at satellite receiver side, due to the used RRM coordination scheme that mitigates interferences.
- Regarding the median curve (in orange) for the intermediate simulated overlapping ratio case (40%):
  - The SINR UL median values decrease also while the distance to the satellite increases,
  - The received SINR at satellite side, is lower whenever not coordinated terrestrial transmission occurs from terrestrial UE which are co-located to NTN UE, and thus, interfere with the NTN uplink.
- Regarding the median curve (in grey) for the worst simulated overlapping ratio case (80%):
  - The SINR UL median values still decrease also while the distance to the satellite increases,
  - The received SINR at satellite side, is drastically lower whenever not coordinated terrestrial transmission occurs from terrestrial UE which are co-located to NTN UE, and thus, interfere with the NTN uplink.

The UE are still sorted by increasing distance from the satellite, from the left to the right of the X-axis. The center of the NTN cell is at 90° elevation angle to the satellite.

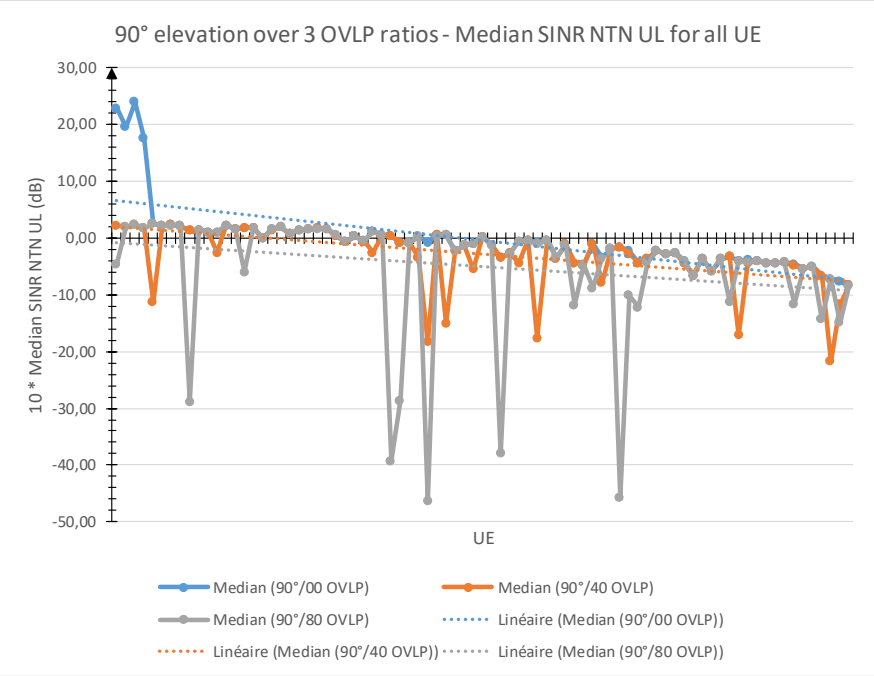

Figure 4-25: NTN SINR UL median curves

As the three curves overlap each other above, alternative views are proposed, in Figure 4-26, Figure 4-27, and Figure 4-28:

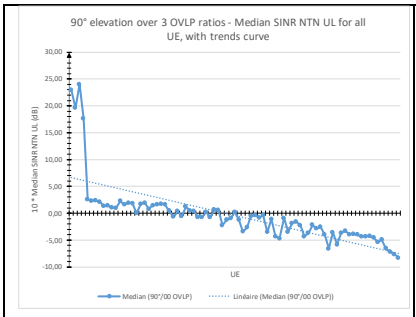

Figure 4-26: Median SINR NTN UL - 90°/ 0% OVLP

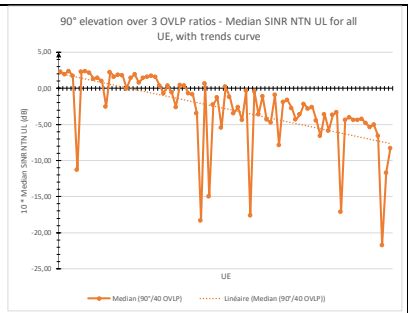

Figure 4-27: Median SINR NTN UL - 90°/ 40% OVLP

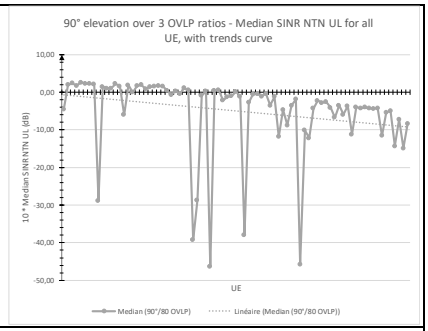

Figure 4-28: Median SINR NTN UL - 90°/ 80% OVLP

As for the previous case, to evaluate more accurately the impact of the RRM coordination scheme to mitigate interferences, Figure 4-29 is proposed, which depicts the measured difference between:

- the median SINRs with 0% overlapping ratio and the median SINRs with the highest tested overlapping ratio (80%), per UE basis and
- the median SINRs with 0% overlapping ratio and the median SINRs with the intermediate overlapping ratio (40%), per UE basis

The trend analysis shows that the difference is very high (SINR lower or even drastically lower) for some NTN uplink. As already said, the reason is that the received SINR at satellite side, is lower whenever not coordinated terrestrial transmission occurs from terrestrial UE which are co-located to NTN UE, and thus, interfere with the NTN uplink.

Note: SINR CDF curves are not available in this case, but they may be generated from raw results.

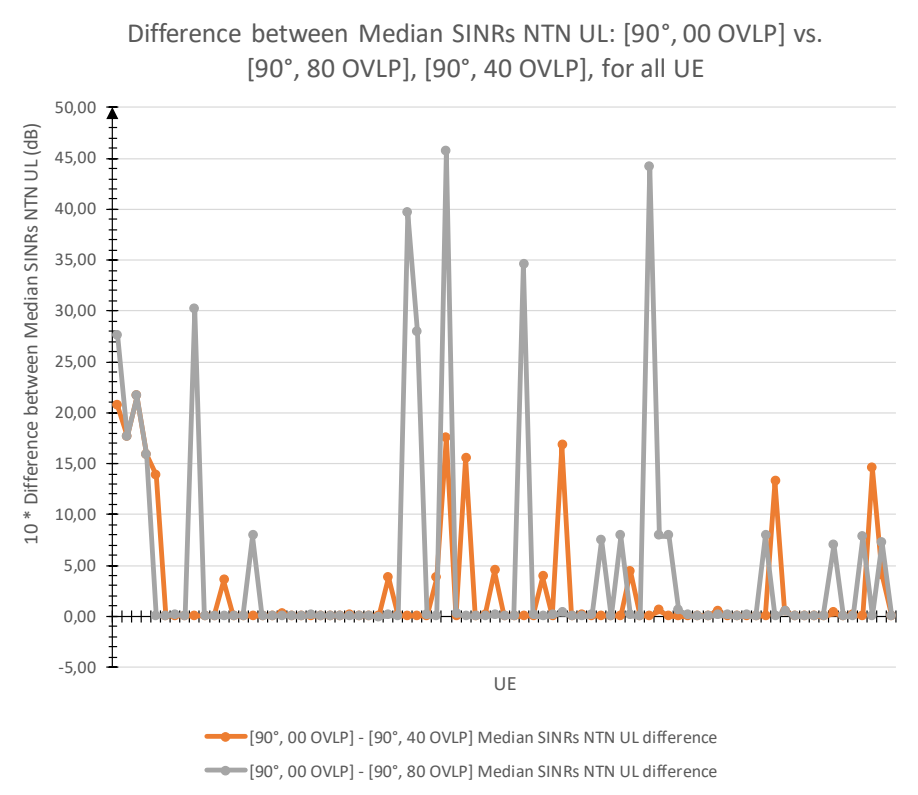

Figure 4-29: Difference between NTN UL SINR curves across different overlapping ratios

4.3.3.3 Terrestrial DL SINR case

As for the previous case, for RRM coordination scheme performance evaluation and trend analysis purposes, three terrestrial DL SINR median curves per overlapping ratio basis, have been reported on the same Figure 4-30:

- The median curve (in blue) for the lowest simulated overlapping ratio (0%) matches the highest SINR values and lowest interference level, but the differences with other curves are small, in particular the orange curve (40% overlapping ratio).
- The median curve (in orange) for the intermediate simulated overlapping ratio case (40%) matches an intermediate interferences level. This curve is closed to the blue one (0% overlapping ratio).
- The median curve (in grey) for the worst simulated overlapping ratio case (80%) matches the lowest SINR values and the highest interferences level. But the SINR values are close to the blue curve SINR values.

The UE are still sorted by increasing distance from the satellite, from the left to the right of the X-axis. The center of the NTN cell is at 90° elevation angle to the satellite.

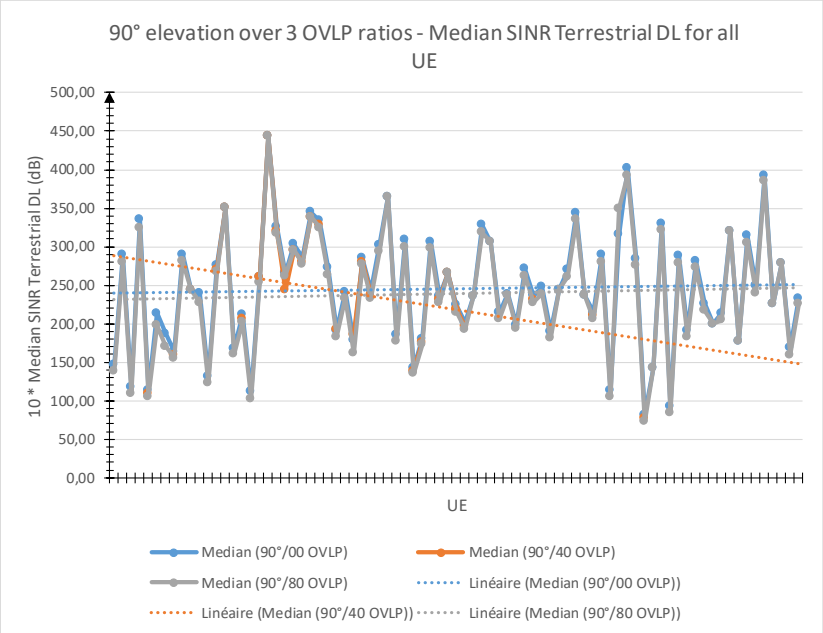

Figure 4-30: Terrestrial SINR DL median curves

As the three curves overlap each other above, alternative Figure 4-31, Figure 4-32 and Figure 4-33 are proposed, for clarification:

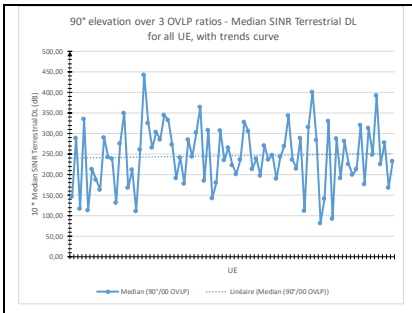

Figure 4-31: Median SINR Terrestrial DL - 90°/ 0% OVLP

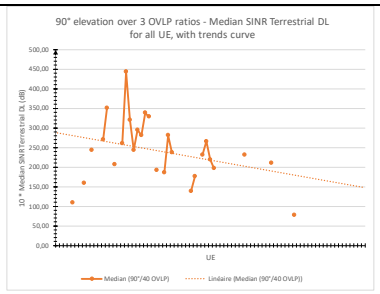

Figure 4-32: Median SINR Terrestrial DL - 90°/ 40% OVLP

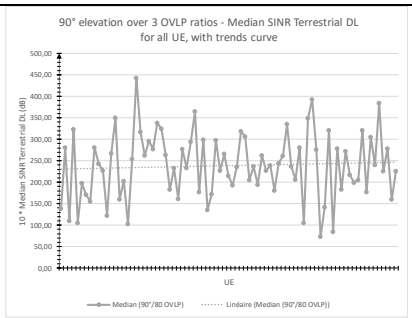

Figure 4-33: Median SINR Terrestrial DL - 90°/ 80% OVLP

As for the previous case, to evaluate more accurately the impact of the RRM coordination scheme to mitigate interferences, Figure 4-34 is proposed, which depicts the measured difference between:

- the median SINRs with 0% overlapping ratio and the median SINRs with the highest tested overlapping ratio (80%), per UE basis and
- the median SINRs with 0% overlapping ratio and the median SINRs with the intermediate overlapping ratio, per UE basis
- The difference values have been multiplied by 10, to see the small differences more accurately

The trend analysis shows that the differences are globally significant but small. Therefore, the benefit of using the RRM coordination scheme to mitigate interferences on terrestrial DL is proven.

Notes:

- SINR CDF curves are not available in this case, but they may be generated from raw results.
- Measurements points are fewer for the 40% overlapping scenario than for the 80% one, due implementation constraints. The related sample must have been reduced.

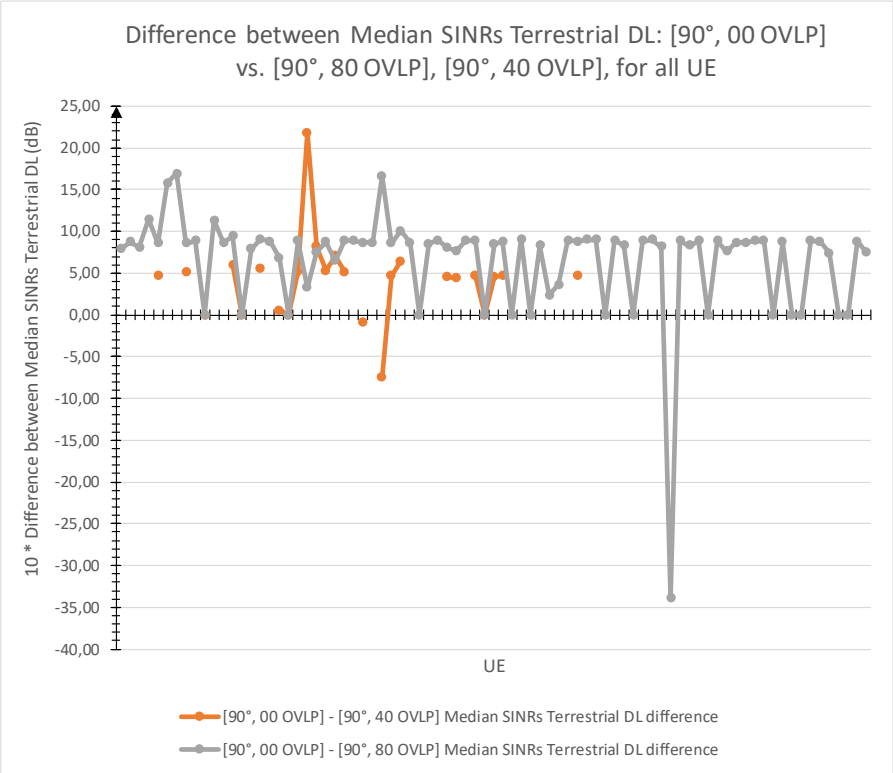

Figure 4-34: Difference between terrestrial DL SINR curves across different overlapping ratios

4.3.3.4 Terrestrial UL SINR case

As for the previous case, the UE are still sorted by increasing distance from the satellite, from the left to the right of the X-axis. The center of the NTN cell is at 90° elevation angle to the satellite. For RRM coordination scheme performance evaluation and trend analysis purposes, three terrestrial UL SINR median curves per overlapping ratio basis, have been reported on the same Figure 4-35:

- Regarding the median curve (in blue) for the lowest simulated overlapping ratio (0 OVLP):
  - The SINR UL median values do not decrease while the distance of the co-located UE to the satellite increases (and reciprocally)
  - The SINR UL median values variations are important
- Regarding the median curve (in orange) for the intermediate simulated overlapping ratio case (40 OVLP):
  - The SINR UL median values decrease also while the distance to the satellite increases
  - The NTN UE co-located to the terrestrial UE seems to not interfere with the terrestrial uplink, at terrestrial base station receiver side
  - The SINR UL median values variations are important
- Regarding the median curve (in grey) for the worst simulated overlapping ratio case (80 OVLP):

- Same trend as for the orange curve but with more measurements points that confirm the trend accuracy

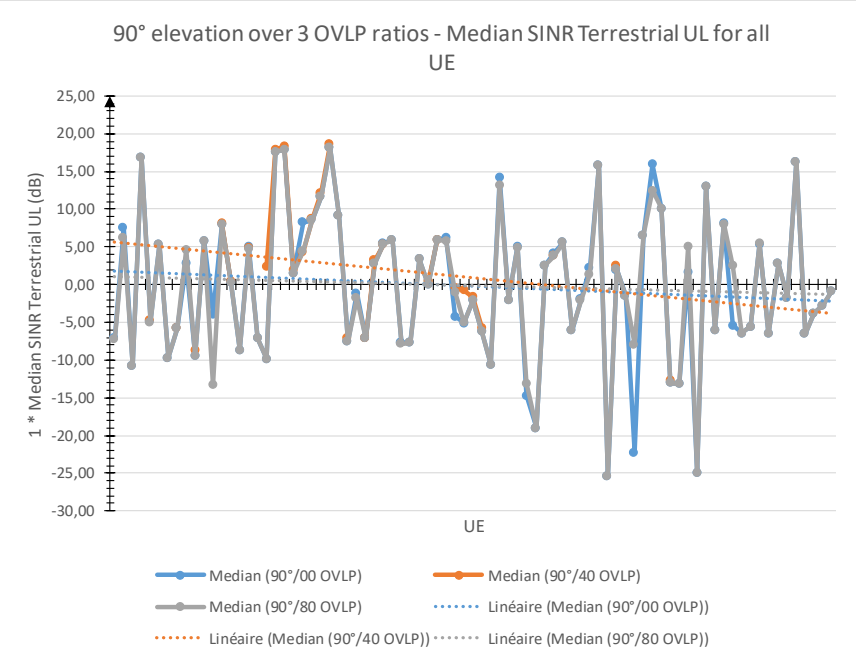

Figure 4-35: Terrestrial SINR DL median curves

As the three curves overlap each other above, alternative Figure 4-36, Figure 4-37, Figure 4-38 are proposed, for clarification. The SINR values scale, on the Y-axis, is multiplied by 20, to make the figures more readable:

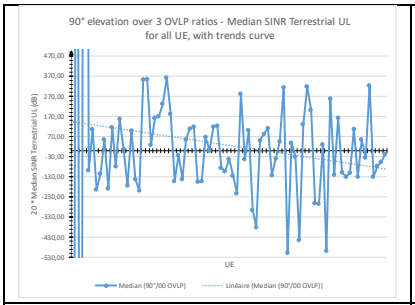

Figure 4-36: 20 * Median SINR Terrestrial UL - 90°/ 0% OVLP

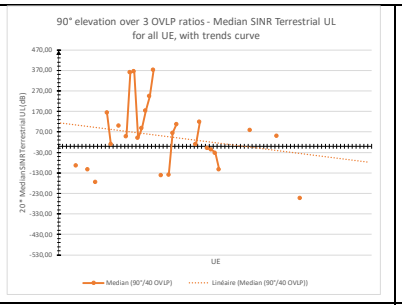

Figure 4-37: 20 * Median SINR Terrestrial UL - 90°/ 40% OVLP

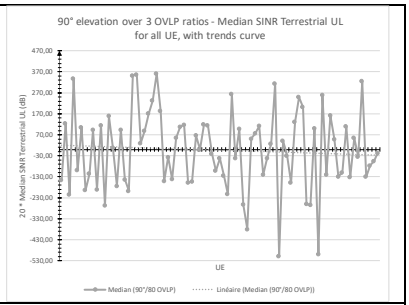

Figure 4-38: 20 * Median SINR Terrestrial UL - 90°/ 80% OVLP

As for the previous case, to evaluate more accurately the impact of the RRM coordination scheme to mitigate interferences, Figure 4-39 and Figure 4-40 are proposed, which depict the measured difference between:

- The median SINRs with 0% overlapping ratio and the median SINRs with the highest tested overlapping ratio (80%), per UE basis and
- The median SINRs with 0% overlapping ratio and the median SINRs with the intermediate overlapping ratio (40%), per UE basis

The trend analysis shows that the difference is very small, excepted high for some not representative UE. We conclude that the tested interference mitigation mechanism has no impact on the terrestrial uplinks.
The reason is that the terrestrial UE are close to their terrestrial base station that receives a stronger signal than the NTN UE interfering signal.

Note: SINR CDF curves are not available in this case, but they may be generated from raw results.

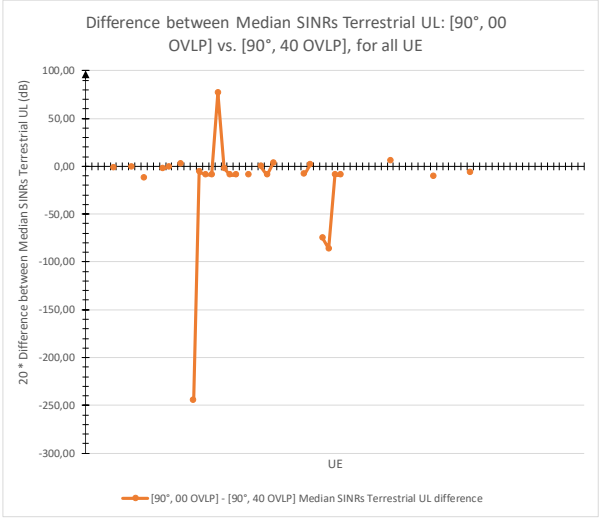

Figure 4-39: 20 * Difference of Median SINR Terrestrial UL [90°/ 0% OVLP] vs. [90°/ 40% OVLP]

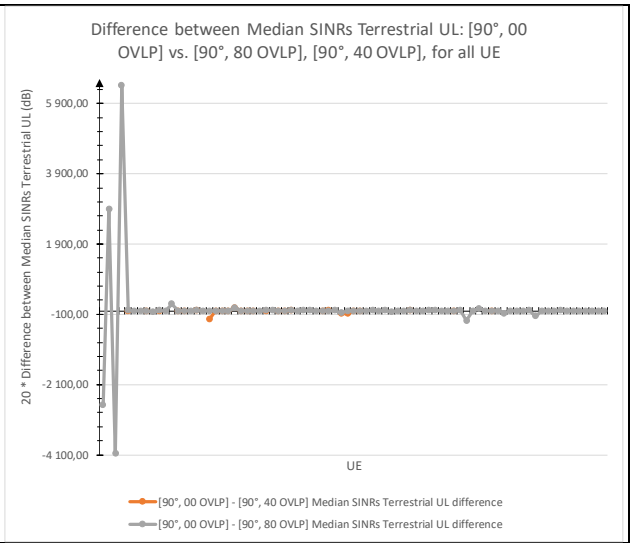

Figure 4-40: 20 * Difference of Median SINR Terrestrial UL [90°/ 0% OVLP] vs. [90°/ 80% OVLP]

4.3.4 Conclusion of the trend analysis

We conclude that:

- The tested RRM coordination scheme has no measured effect on the terrestrial uplinks.
- This RRM coordination scheme is relevant for all the NTN downlinks, NTN uplinks and terrestrial downlink, for interference mitigation purposes.
- It is more effective for interference mitigation, on NTN downlinks and terrestrial downlinks.
- The efficiency of the RRM coordination scheme is more efficient when the UE are closer to the satellite. However, the more distant UE also benefit from the RRM coordination scheme.

4.4 Recommendations for the WP5 test bed

Recommendations have been made, to coordinate the Radio Resource Management of both terrestrial and NTN systems, with one coordination mechanisms type amongst:

- RRM coordination by splitting the resource into time * frequency clusters, such as ICIC (Inter-cell Interference Coordination), at PRB level
- RRM coordination by splitting the resource into clusters of sub-carriers, such as Carrier Aggregation (CA) with cross-carrier scheduling
- RRM coordination by splitting the resource into sub-band clusters

The splitting of resource into time cluster, such as ABS (Almost Blank Sub frames) or ZP (Zero Power) frames had been rejected in primary analysis, due the deep impact on the MAC scheduler required to implement them.

The solution based on resource splitting into sub-band clusters has been selected by WP5, as no other type of coordination but this one could be supported by WP5 sub-systems.

5 Conclusion

In Section 2, we proposed a dual beamforming technique for interference mitigation in order to support the coexistence of the satellite and cellular networks. The dual beamforming technique combines the MRT and ZF beamforming techniques, so that interference to the satellite Earth station is sufficiently mitigated while enhancing the sum rate of the cellular network. Adaptive allocation of the allowable interference level to each base station is also proposed for further improvement of the sum rate of the cellular network. The proposed dual beamforming technique is shown to outperform the conventional MRT and ZF-only beamforming schemes.

It has been shown in section 3 that interference from a terrestrial system on a satellite system adjacent in frequency can be efficiently managed by using a filtered waveform like BF-OFDM. BF-OFDM allows to limit the guard bands between both systems, therefore resulting in a net throughput gain. Furthermore, BF-OFDM is fully 5G NR compliant and suitable to satellite-terrestrial multi-connectivity, thanks to its bandwidth configurability.

In Section 4.1, a resource allocation scheme was proposed, which can adaptively turn the transmission of the cellular base stations on and off, in order to protect the satellite Earth station. The proposed scheme was implemented by using the non-circular-shaped exclusion zone, which determines the radius of the exclusion zone considering the transmit/receive beam directions of the cellular base station and the satellite Earth station, respectively. Performance gain by the proposed scheme over the conventional circular-shaped exclusion zone was evaluated by computer simulation.

Section 4.2 discussed mechanisms to mitigate interferences between terrestrial RANs and NTN RAN, based on RRM coordination schemes. One of these mechanisms was assessed in section 4.3. Therefore, a RRM coordination scheme simulator has been developed and campaign tests were performed. The tested RRM coordination scheme (see annex 8.2), based on PRBs allocation to disjoint cell clusters, operates in time*frequency domains, and is relevant for all the NTN downlinks, NTN uplinks and terrestrial downlink, to mitigate interference. It could also be known that it has no effect on the terrestrial uplinks.

The results from this deliverable are expected to contribute to the on-going and planned works of the project with the following details:

- Results from the proposed dual-beamforming technique showed that a significant interference reduction can be achieved through beam management techniques. Although in a much simpler form, a beamforming technique will be employed in the KR cellular testbed implementation, i.e., beam switching, which can be used to maximize the received signal quality while minimizing the effects of interference (if any) and noise.
- The BF-OFDM waveform is being implemented in the terrestrial hardware modem for integration in the EU testbed and trial platform.
- Recommendations for selecting RRM coordination schemes for WP5 test bench have been made in the RRM coordination schemes preliminary analysis. An RRM coordination scheme (algorithm), based on Hard Frequency Reuse, in FDD mode, radio resource partitioning into two sub-band clusters has been selected for implementation in the WP5. The bandwidth of the terrestrial and NTN sub-bands are configurable.

6 References

[1] C. Zhang, C. Jiang, L. Kuang, J. Jin, Y. He, and Z. Han, “Spatial spectrum sharing for satellite and terrestrial communication networks,” IEEE Trans. Aerosp. Electron. Syst., vol. 55, no. 3, Jun. 2019.

[2] A. Mohamed, B. Evans, “Spectrum sharing framework for 5G cellular system and satellite services,” in Proc. 25th Ka-band communication, navigation and earth observation conference, Sorrento, Italy, Oct. 2019.

[3] S. K. Sharma, S. Chatzinotas, and B. Ottersten, “Transmit beamforming for spectral coexistence of satellite and terrestrial networks,” in Proc 2013 8th International Conference on Cognitive Radio Oriented Wireless Networks (CROWNCOM), Washington, DC, 2013, pp. 275-281.

[4] M. A. Vazquez, L. Blanco, and A. I. Perez-Neira, “Spectrum sharing backhaul satellite-terrestrial systems via analog beamforming,” IEEE J. Sel. Topics Signal Process., vol. 12, no. 2, May 2018.

[5] M. Lin, Z. Link, W.-P. Zhu, and J.-B. Wang, “Joint beamforming for secure communication in cognitive satellite terrestrial networks,” IEEE J. Sel. Topics Signal Process., vol 36, no. 5, May 2018.

[6] C. Liu, W. Feng, Y. Chen, C.-X. Wang, and N. Ge, “Optimal beamforming for hybrid satellite terrestrial networks with nonlinear PA and imperfect CSIT,” IEEE Wireless Commun. Lett., vol. 9, no. 3, Mar. 2020.

[7] RECOMMENDATION ITU-R S.465-5, “Reference earth-station radiation pattern for use in coordination and interference assessment in the frequency range from 2 to about 30 GHz,” 1993.

[8] 3GPP TR 38.901, “3rd Generation Partnership Project; Technical Specification Group Radio Access Network; Study on channel model for frequencies from 0.5 to 100 GHz (Release 14),” v14.0.0, Tech. Rep., 2017.

[9] 3GPP TR 38.801, “3rd Generation Partnership Project; Technical Specification Group Radio Access Network; Study on new radio access technology: Radio access architecture and interfaces (Release 14),” v14.0.0, Tech. Rep., 2017.

[10] 3GPP TR 38.811, “3rd Generation Partnership Project; Technical Specification Group Radio Access Network; Study on New Radio (NR) to support non-terrestrial networks (Release 15),” v15.1.0, Tech. Rep., 2019.

[11] 3GPP TR 38.821, “3rd Generation Partnership Project; Technical Specification Group Radio Access Network; Solutions for NR to support non-terrestrial networks (NTN) (Release 16),” v1.0.0, Tech. Rep., 2019.

[12] Project Proposal: 5G ALL-STAR (Technical Annex); Research and Innovation Actions; Part B – Technical Annex Section 1-3

[13] 5G-ALLSTAR D3.1, “Spectrum usage analysis and channel model”, June 2019.

[14] 5G-ALLSTAR D3.2, “Interference analysis for terrestrial-satellite spectrum sharing”, December 2019

[15] CADSAT-Carrier Aggregation in Satellite Communication Networks, Ref. https://artes.esa.int/projects/cadsat

[16] 3GPP; TS Group RAN; Study on NR Access Technology; Physical Layer Aspects (Release 14), 2017, 3GPP TR 38.802 V14.2.0 (2017-09)

[17] Demmer, David, et al. "Block-Filtered OFDM: a novel waveform for future wireless technologies." 2017 IEEE International Conference on Communications (ICC). IEEE, 2017.

[18] R. Zakaria and D. L. Ruyet, “A novel FBMC scheme for Spatial Multiplexing with Maximum Likelihood detection,” in Wireless Communication Systems (ISWCS), 2010 7th International Symposium on, Sept 2010, pp. 46

[19] R. Gerzaguet, D. Demmer, J.-B. Dore, and D. Kténas, “Block-Filtered ´ OFDM: a new promising waveform for multi-service scenarios,” in Proc. IEEE ICC 2017 Wireless Communications Symposium (ICC’17 WCS), Paris, France, May

[20] Tani, Khaled, et al. "PAPR reduction of post-OFDM waveforms contenders for 5G & Beyond using SLM and TR algorithms." 2018 25th International Conference on Telecommunications (ICT). IEEE, 2018.

[21] C. Zhang, C. Jiang, L. Kuang, J. Jin, Y. He, and Z. Han, “Spatial spectrum sharing for satellite and terrestrial communication networks,” IEEE Trans. Aerosp. Electron. Syst., vol. 55, no. 3, pp. 1075-1089, Jun. 2019.

[22] G. Hattab, P. Moorut, E. Visotsky, M. Cudak, and A. Ghosh,“Interference Analysis of the Coexistence of 5G Cellular Networks with Satellite Earth Stations in 3.7-4.2GHz,” in Proc. IEEE Int. Conf. Commun. (ICC) Workshops, May 2018.

7 Appendix A - Mapping between WP3 objectives and the D3.3 chapters

Table 7-1: Mapping between WP3 objectives and the D3.3 chapters

Chapter	Covered WP3 objectives, amongst O3.5, O3.6, O3.7 (see NOTE)
2. Dual beam forming technique for interference mitigation	O3.5, O3.7
3. Signal processing techniques for active interference mitigation	O3.5, O3.7
4. Interference mitigation through RRM	O3.6, O3.7
4.2. Exclusion region design for interference mitigation	O3.6, O3.7
4.3. Coordinated RRM schemes	O3.6, O3.7
Performance evaluation of a RRM colorization scheme, based on simulations	
8. Appendix B - RRM simulator key functions and NS-3 key adaptations	O3.7
NOTE: According to [12], the WP3 objectives that D3.3 should address are: **O3.5:** Develop signal processing technologies to mitigate co-channel / adjacent interference **O3.6:** Develop Radio Resource Management scheme to mitigate inter access interference **O3.7:** Analyse and assess the performance of the developed interference mitigation techniques	

8 Appendix B - RRM simulator key functions and NS-3 key adaptations

8.1 Overview

TAS has developed a system level simulator that allows for the simulation of interference scenarios between multiple radio access technologies (cellular and satellite) sharing the same spectrum in frequency bands below 6 GHz (3GPP Frequency Range no.1 : FR1), such as S-Band, and a part of C-band, at a resource management level.

This simulator is designed to host several resource management algorithms, for mitigating the interference while maximizing the overall throughput and the user QoS.

Optimal implementation approaches in the 5G system of the joint cellular/satellite RRM is researched.

The simulator has been designed to evaluate the efficiency of the RRM algorithm, across several NTN / Terrestrial Cells overlapping ratios: 80% (high overlapping), 40% (medium overlapping) and 0% (no overlapping, thanks to a RRM algorithm which is expected to mitigate interferences between both NTN and terrestrial systems.

For development constraints reasons, only one RRM algorithm has been implemented, in time * frequency domain, tested and operated for results analysis.

8.2 Implemented RRM algorithm

The implemented RRM algorithm is an Inter-cell Interference Coordination like mechanism, based on disjoint resource clusters, at PRBs (RBGs in fact) basis, one cells cluster being associated to a repeatable color pattern.

As depicted in Figure 8-1:

- For both UL and DL, the same resource allocation GRID, at PRB level, is applied to all terrestrial, non-terrestrial gNBs.
- Cells are grouped by cluster, with 1 color per cluster basis, for a Bandwidth of 100 PRBs (5G Physical Resource Blocks).
- Two adjacent cells, if served by different gNBs, cannot belong to the same resource cluster.
- Two adjacent resource clusters cannot have the same color.
- Terrestrial Cells of the same cluster can re-use the same color provided they are not adjacent.

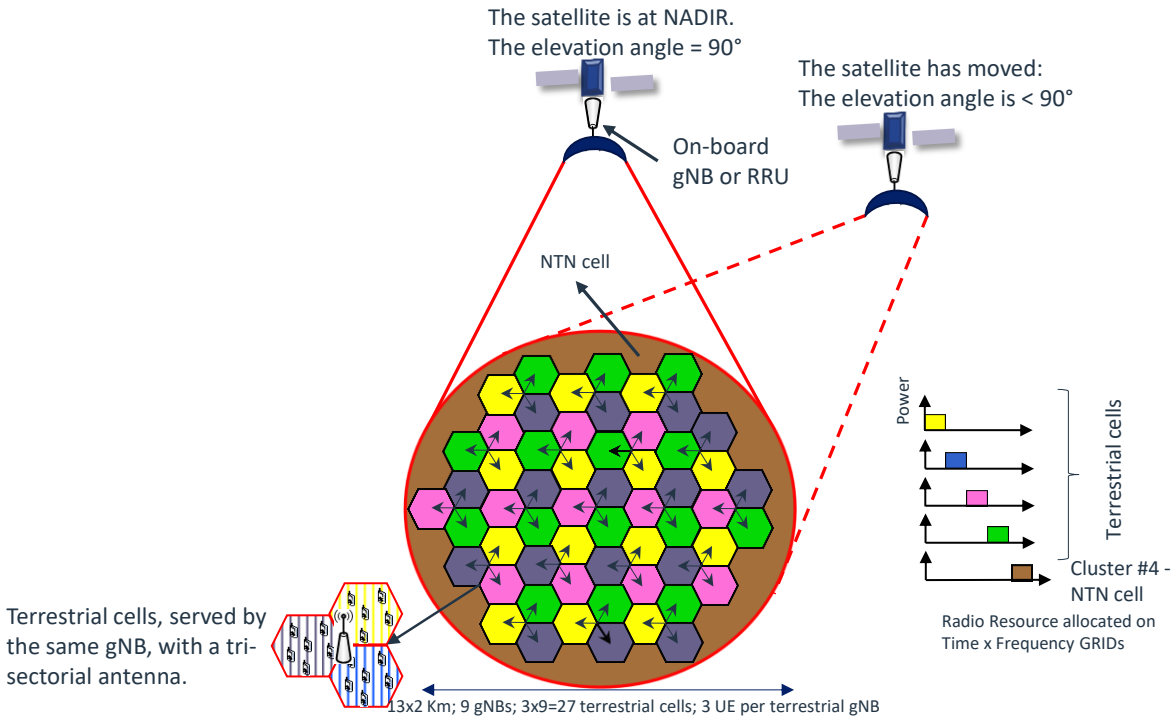

Figure 8-1: Implemented RRM algorithm – Overview

The RRM coordination scheme for the downlink and the uplink cases is depicted in Figure 8-2 and Figure 8-3. There is no resource overlapping between the NTN cell and the Terrestrial Cell. SINR have been measured, by simulations at both NTN receivers and terrestrial receiver sides, to measure the efficiency of the RRM coordination, compared to scenarios with 40% and 80% of radio resource overlapping.

Note that in the simulator, a Downlink RBG contains 4 PRBs and an uplink RBG contains 1 PRB.

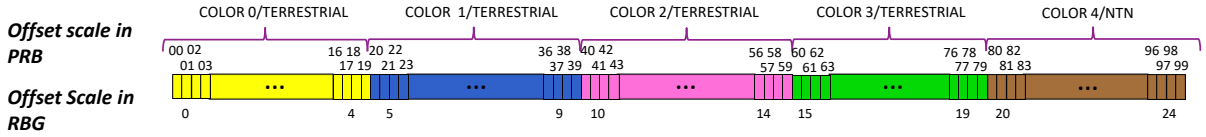

Figure 8-2: Implemented RRM scheme - Downlink case - No overlapping

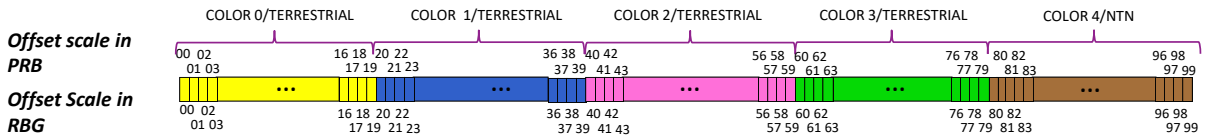

Figure 8-3: Implemented RRM scheme - Uplink case - No overlapping

The RRM coordination scheme performance is evaluated through several scenarios with different elevation angles and compared to the situation without through several scenarios with no coordination but different resource overlapping ratios, between non-terrestrial cell and terrestrial cells:

- For both UL and DL, the same resource allocation GRID, at PRB level, is applied to all terrestrial gNBs and non-terrestrial gNBs
- Cells are still grouped by cluster, with 1 color per cluster basis, for a Bandwidth of 100 PRBs (5G Physical Resource Blocks)
- Two adjacent clusters may transmit on the same PRB(s), according to a given overlapping ratio (40%, 80%), per scenario basis. In other words, there is no band guard anymore, between the NTN cluster and the terrestrial clusters: they overlap each other.

The absence of RRM coordination scheme with a 40% overlapping ratio for the downlink and the uplink cases is depicted in Figure 8-4 and Figure 8-5.

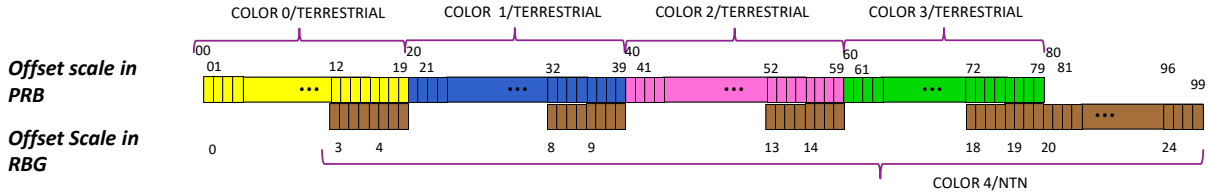

Figure 8-4: No coordination RRM scheme - Downlink case – 40% overlapping ratio

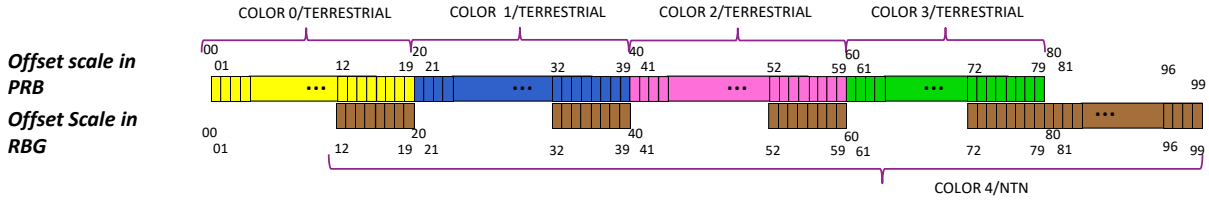

Figure 8-5: No coordination RRM scheme - Uplink case – 40% overlapping ratio

8.3 Other candidate, not-implemented RRM algorithms

As discussed in 4.2, other basic RRM algorithms in frequency domain (disjoint frequency cluster), could be implemented provided additional development. RRM in time domain only (disjoint transmitted sub-frames clusters), such as ABS (Almost Blank Sub-frame) or ZP (Zero Power) sub-frames requires a deep modification of the NS-3 MAC layer scheduler.

8.4 Configurable Cells Overlapping between NTN and terrestrial systems

The overlapping ratios are configurable, per simulation scenario basis.

In the simulator, NTN and terrestrial cells overlap whenever a Terrestrial cell (respectively a NTN cell) transmits on the same PRBs (Time * Sub-carriers) than the NTN cell (respectively than some terrestrial cells). Cells Overlapping are simulated for each direction: DL, UL.

The effects of each overlapping ratios are measured in terms of SINR and measured SINR are discussed across different overlapping ratios scenarios.

8.5 NS-3 Cellular system simulator basic platform

NS-3 is a discrete event simulator, proving several modules, including LTE module, that suits frequency bands below 6GHz.

Its main characteristics are listed below:

- Terrestrial simulation of 4G/5G networks
- End to End simulation: UE <-> Base Station <-> Core Network with
- Realistic Data, Control Planes Protocol stacks models (MAC, RLC, PDCP, S1-U, X2-U).
- The satellite can be positioned on any orbit and altitude. The satellite mobility is implemented but disabled by default.
- UE are uniformly distributed on earth over a configurable studied area, under one satellite-beam coverture
- Re-use of NS-3 antenna models:
    - Cosine model, for the terrestrial base station
    - Isotropic model for the UE
- Implementation of a satellite antenna model, based on a Bessel diagram
- Configurable Satellite-Earth propagation delay
- Re-use of NS-3 LTE channel model. 5G radio interface is modeled, in a “LTE compatible mode”: re-use of the Transmission bandwidth model, the PRB model, 15 KHz SCS. Only FDD mode is modeled

The simulation has modeled:

- One NTN base station, 28 terrestrial base stations and 82 hybrid UE
- An hybrid UE is a couple of UE: one NTN UE served by the NTN base station and positioned at the same place as a terrestrial UE served by one terrestrial base station.

8.6 Modifications the NS-3 cellular system simulator to suit NTN constraints

The NS-3 simulator has been modified in a separate branch, as described in the following chapters.

8.6.1 Features added in an external module, as a NS-3 library

The following features have been added:

- **Satellite mobility model**
    - Frozen satellite trajectory given an altitude, an elevation angle and a beam center (in latitude and longitude).
    - The satellite position is configurable, wrt to this trajectory
- **Propagation Loss Model**
    - For NTN channel: Handling of large scale model, wrt 3GPP TR 38.811 [10] for satellite, that takes into account:
        - Free space loss
        - Shadow fading (see 8.7.4)
        - Atmospheric path loss
    - For terrestrial channel: Handling of 3GPP Propagation loss model for terrestrial wrt 3GPP TR 38.901 [8]
    - Selection of the propagation model, depending on the type of network entity (Terrestrial or NTN)
    - Note that only LoS (Line of Sight) mode is implemented
- **Terrestrial gNB antenna model**

- A tri-sectorial antenna model has been used for the terrestrial base station.
- NS-3 cosine antenna model has been adapted to work in 3D space on Earth

- **New model of NTN satellite antenna, based on Bessel model, 2m diameter**
- **An RRM algorithm, for interference mitigation purposes**
  - 3GPP ICIC scheme like, based on PRBs allocation per cells cluster
  - with a radio resource reuse pattern (FRF=4 for terrestrial cells + 1 for satellite)
- **Miscellaneous**
  - Helper to generate raw data for heat map post processing
  - Helper to see the scenario in Cesium JS (Java Script)
  - Generic configurable scenario to run simulations
  - Scenario generator tool
  - Input file readers (user positions, configurations…)
  - Geometry, mathematics and geospatial utilities. The distance and the channel propagation delay have been adapted to suit NTN constraints and a 3D world, instead of the NS-3 2D model.
  - Implementation of post processing scripts to generate KPI, curves and heat maps, from NS-3 raw outputs.

8.6.2 Features modified in the core of NS-3

The following core NS-3 features have been modified, related to the signalization at the radio interface:

- The SRS (Sounding Reference Signal) has been split for computation purposes*
- The SRS was over the whole band (100 PRBs).
- In the RRM simulator, it is computed based on the used PRBs, both NTN PRBs or Terrestrial PRBs, depending on the link type.

8.6.3 Encountered Issues

The following main issues have been encountered and fixed:

- Investigations have been carried out to understand how the link budget was computed in NS-3 mobile module, to adapt it to the satellite budget link case.
- In NS-3 mobile module, the SRS is computed by default over the whole band. It suits to terrestrial base stations but it does not for the satellite (NTN) base station. The power distributed fairly in uplink on each PRB is not high sufficient to transmit the signal. This issue was difficult to analyze and fix, as the default observable was only a bad C/(N+I) on the data channel. But the real issue came from the signaling channel, that affected the low protocol layers (Physical and MAC), between the satellite base station and the UE. In the NS-3 core, the SRS computation had to be adapted to take into account a restricted amount of PRBs.
- An array antenna model for the terrestrial gNBs was implemented, tested and the conclusion led to reject this model, as it was not suitable to the RRM scenarios, modeling a large amount of UE to be connected and served by their gNB, connect (82 UE), to get relevant statistical results. The antenna gain was measured with such model and it was generally very bad or even non-existent on the edges of the sectors. Finally, the tri-sectorial antenna model was selected for the terrestrial gNBs in the RRM simulator, that is the default model in NS-3 mobile module, for frequency bands below 6 GHz.

- A lot of raw outputs have been processed but this post-processing was not completely automatic. More post-processing scripts should have been budgeted and developed, to produce statistical results, which would have avoided tedious, time consuming operations with a digital spreadsheet.

8.7 Setting up the transmission and reception at physical layer for all the scenarios

The parameters for modeling the transmission and the reception, at the radio interfaces, between the satellite and the NTN UE and between the terrestrial gNBs and the terrestrial UE, are described in the following chapters.

8.7.1 Frequency bands, SCS, PRB size

The used UL, DL frequency bands and the SCS are described in Table 8-1.

Table 8-1: Used frequency bands and SCS

Parameter	Unit	Value
Downlink Frequency	GHz	2.11
Uplink Frequency	GHz	1.92
SCS	KHz	15
PRB size	KHz	180
Bandwidth	KHz	18 000
Division Duplexing mode (FDD vs. TDD)		FDD

8.7.2 Main parameters for transmission

The main parameters related to the transmission, are described in Table 8-2:

Table 8-2: Main parameters for transmission

Entity	Antenna max gain	Tx Power
NTN UE (Tx)	0 dB	23 dBm (200 mW)
Terrestrial UE (Tx)	0 dB	23 dBm (200 mW)
Satellite (Tx)	30 dBi	46 dBm (39 W)
Terrestrial gNB (Tx)	5 dB	46 dBm (39 W)

8.7.3 Main parameters for reception

The main parameters related to the reception, are described in Table 8-3

Table 8-3: Main parameters for reception

Entity	Noise Figure	Antenna Temperature	Antenna max gain
NTN UE (Rx)	7 dB	290 K	0 dB
Terrestrial UE (Rx)	7 dB	290 K	0 dB
Satellite (Rx)	4.27 dB	290 K	30 dBi
Terrestrial gNB (Rx)	5 dB	290 K	5 dB

8.7.4 Shadow fading

According to TR38.811 [10] (chapter 6.2.2), the following shadow fading has been implemented. The 90° elevation angle and sub-urban scenario have been used for the simulation scenarios.

Table 8-4: Shadow fading – Suburban and rural scenario

Suburban & rural scenario		
Elevation(°)	**Sigma(dB)**	**Shadowing (dB)**
10	1.79	4.164162695
20	1.14	2.652036576
30	1.14	2.652036576
40	0.92	2.140240044
50	1.42	3.303413981
60	1.56	3.629102684
70	0.85	1.977395693
80	0.72	1.674970469
90	0.72	1.674970469

Table 8-5: Shadow fading – Urban (dense) scenario

Urban (dense) scenario		
Elevation(°)	**Sigma(dB)**	**Shadowing (dB)**
10	3.5	8.142217559
20	3.4	7.909582772
30	2.9	6.746408835
40	3	6.979043622
50	3.1	7.21167841
60	2.7	6.28113926
70	2.5	5.815869685
80	2.3	5.35060011
90	1.2	2.791617449